Applied Network Science

RESEARCH

Open Access

An efficient weighted network centrality approach for exploring mechanisms of action of the Ruellia herbal formula for treating rheumatoid arthritis

Peter Juma Ochieng[1,2*†], Abrar Hussain[1†], József Dombi[1†] and Miklós Krész[3,4,5†]

†All authors contributed equally

*Correspondence:
Juma@inf.u-szeged.hu

[1] Institute of Informatics, University of Szeged, Árpád tér, Szeged 6720, Hungary
[2] Bánki Faculty, Obuda University, Bécsi str, Budapest 1034, Hungary
[3] InnoRenew CoE, Livade 6, 6310 Izola, Slovenia
[4] Andrej Marušič Institute, University of Primorska, Muzejski trg 2, 6000 Koper, Slovenia
[5] Department of Applied Informatics, University of Szeged, Boldogasszony sgt. 6, Szeged 6725, Hungary

Abstract

Aim: This study outlines an efficient weighted network centrality measure approach and its application in network pharmacology for exploring mechanisms of action of the *Ruellia prostrata* (RP) and *Ruellia bignoniiflora* (RB) herbal formula for treating rheumatoid arthritis.

Method: In our proposed method we first calculated interconnectivity scores all the network targets then computed weighted centrality score for all targets to identify of major network targets based on centrality score. We apply our technology to network pharmacology by constructing herb-compound-putative target network; compound-putative targets-RA target network; and imbalance multi-level herb-compound-putative target-RA target-PPI network. We then identify the major targets in the network based on our centrality measure approach. Finally we validated the major identified network targets using the enrichment analysis and a molecular docking simulation.

Result: The results reveled our proposed weighted network centrality approach outperform classical centrality measure in identification of influential nodes in four real complex networks based on SI model simulation. Application of our approach to network pharmacology shows that 57 major targets of which 33 targets including 8 compositive compounds, 15 putative target and 10 therapeutic targets played an important role in the network and directly linked to rheumatoid arthritis. Enrichment analysis confirmed that putative targets were frequently involved in TNF, CCR5, IL-17 and G-protein coupled receptors signaling pathways which are critical in the progression of rheumatoid arthritis. The molecular docking simulation indicated four targets had significant binding affinity to major protein targets. Glyceryl diacetate-2-Oleate and Oleoyl chloride showed the best binding affinity to all targets proteins and were within Lipinski limits. ADMET prediction also confirm both compounds had no toxic effect on human hence potential lead drug compounds for treating rheumatoid arthritis.

Conclusion: This study developed an efficient weighted network centrality approach as tool for identification of major network targets. Network pharmacology findings provides promising results that could lead us to design and discover of alternative drug

compounds. Though our approach is a purely in silico method, clinical experiments are required to test and validate the hypotheses of our computational methods.

Keywords: Network centrality, Rheumatoid arthritis, *Ruellia*

Introduction

Rheumatoid arthritis is an autoimmune disease characterized by pain and synovial inflammation that may result in the destruction of cartilage and bone. Recently, a study has reported a rheumatoid arthritis prevalence of 1% and it affects three times more women than men (Anderson et al. 2012; Smolen et al. 2003; Scherer et al. 2020). Understanding the etiology of rheumatoid arthritis remains an active area in medical research. Studies have shown that rheumatoid arthritis is a multi-factorial disease probably caused by genetic predispositions or environmental factors (Li et al. 2022; Kour et al. 2022). Developments of alternative drugs to treat and cure rheumatoid arthritis are still out of our reach, and the development of new therapeutic anti-rheumatic drugs with minimal or no side-effects is a great challenge (Koller et al. 2019; Martin et al. 2013; Chakravarty et al. 2008). Although remedies such as non-steroidal anti-inflammatory drugs (NSAIDs) (Kelleni 2021), corticosteroids (Kapugi and Cunningham 2019; Hodgens and Sharman 2021), disease-modifying anti-rheumatic drugs (DMARDS) (Grove et al. 2001), and biologic response modifiers ('biologicals') (Hazlewood et al. 2016) have been used in the management and treatment of rheumatoid arthritis, some of these remedies have adverse side effects (Tóth et al. 2022; Chakravarty et al. 2008). Therefore, it is necessary to develop alternative drugs with minimal or no side effects for the treatment of rheumatoid arthritis. Recently the use of ayurvedic drugs has gained popularity in clinical research. For instance, a study has shown that *Ruellia prostrata* (RP) and *Ruellia bignoniiflora*(RB) herbal medicine and its constituents could have anti-inflammatory and anti-analgesic properties (Dogan et al. 2022, 2022; Weyand and Goronzy 2021). However, the identification and elucidation of *Rueilla* active constituent compositive compounds and their molecular mechanism of action in treating of rheumatoid arthritis remain unknown (Smolen et al. 2003; Chothani et al. 2010; Arirudran et al. 2011). To understand the relationship of interacting components such as drugs, genes, proteins, and disease targets computational methods like network biology, system biology, polypharmacology, and network pharmacology have been recently proposed (Yuan et al. 2021; Yu et al. 2018; Zhou et al. 2020). These methods apply omics and system biology strategies to decipher the underlying mechanism of action and synergetic effect of multiple targets and multiple components via a network analysis (Wan et al. 2019; Xin et al. 2021). In general, network pharmacology is widely based on network construction techniques, a network analysis and database quarry techniques which provides a preliminary understanding of the mechanism of action at the system level (Nogales et al. 2021; Niu et al. 2021). Recently, modeling the drug-target interaction in complex biological systems has attracted the attention of medical researchers (Wachi et al. 2005; Zhou et al. 2020; Xin et al. 2021). In network pharmacology these complex biological system are often presented as complex networks with heterogeneous components that are quantified by a network centrality measure approach (Reia et al. 2017). Though several studies in network pharmacology applied traditional centrality

measures approaches to investigate the important network components these methods often depend on the network structure and this makes them less efficient when handling with complex dynamic network systems and the area of application (Özgür et al. 2008; Rodrigues et al. 2016; Brandes 2001). Thus,in this study, we developed an efficient weighted network centrality measure approach for exploring mechanisms of action of the *Ruellia prostrata* and *Ruellia bignoniiflora* herbal formula for treating rheumatoid arthritis. The rest of this paper is organized as follows. In Section Materials and methods, we describe our new approach for calculating the interconnectivity score and weighted network centrality and its application in network pharmacology. In Section Calculation of the network-based interconnectivity score, we present and interpret our results. In Section Calculation of weighted network centrality, we discuss our findings and then we draw some pertinent conclusions.

Materials and methods

Now, we will describe the our new proposed approach for the calculation of the interconnectivity score and weighted centrality measures for the identification of major network components and its application in network pharmacology.

Calculation of the network-based interconnectivity score

We propose a general approach for the calculation of the interconnectivity score among network components. This approach is a local network-based approach that prioritizes network nodes based on their overall connectivity to other nodes in the network. In our calculations we made the following assumptions: (1) there is a direct interaction between a pair of nodes; (2) there are indirect interactions with a path length of two network nodes which we call the shared neighborhood of the two nodes; (3) the network is a tripartite network consisting of nodes i, j and k. Thus, we can calculate interconnectivity using the following:

$$I(i,k) = e(i,k)\left(\frac{2+\left|N(i)\cap N(k)\right|}{\sqrt{deg(i)\,deg(k)}}\right), \tag{1}$$

where $I(i,k)$ is the interconnectivity between nodes i and k, $deg(i)$ and $deg(k)$ is the degrees of node i and k respectively and N is the size of the shared neighborhood connectivity. Here,

$$e(i,k) = \begin{cases} 1 & \text{if an edge exists between } i \text{ and } k \\ 0 & \text{otherwise} \end{cases} \tag{2}$$

$e(i, k)$ is the edge between node i and k. Therefore, using Eq. (1) the interconnectivity score of node j directly interacting with node i and k in their shared neighborhood can be calculated using

$$s(j) = \frac{1}{|DEG|}\sum_{k\in DEG(j)} e(i,k)\left(\frac{2+\left|N(i)\cap N(k)\right|}{\sqrt{deg(i)\,deg(k)}}\right), \tag{3}$$

where $s(j)$ is the interconnectivity score of node j with respect to node k and DEG represents the degree of all set of node k.

Calculation of weighted network centrality

Using the interconnectivity score $s(j)$ calculated above, we can introduce a new approach for computing the weighted centrality measure based on the traditional centrality measure such as degree centrality, closeness centrality, and betweenness centrality shown in Fig. 1.

Weighted degree centrality

Freeman's (1978) degree centrality is defined as the total number of connections or edges attached to the node with respect to other nodes in the network (Dörpinghaus et al. 2022) and it usually calculated by

$$C^D(i) = \sum_{\substack{j=1 \\ j \neq i}}^{|N|} e(i,j), \tag{4}$$

where $C_D(i)$is the degree centrality of node i, $e(i,j)$is the edge connecting nodes i and j is 1 if it exists otherwise it is 0, and N is the total number of nodes in the network. Therefore using Eqs. (2) and (3), the degree weight of node j is given by

$$w^{DC}(j) = \frac{s(j)\sum_{k=1}^{n_1} e(j,k)}{\ln\left(\sum_{k=1}^{n_1} e(j,k)\right)}, \tag{5}$$

where $w^{DC}(j)$ is the degree weight of node j, $e(j,k)$ represents the edge between nodes j and k whose value is 1 if it exists otherwise it is 0, and n_1 is total number of nodes k in the network. Therefore, using Eq. (4) the weighted degree centrality score of the network node i can be calculated using

$$\phi^{DC}(i) = \sum_{j=1}^{n_2} w^{DC}(j) e(i,j) \tag{6}$$

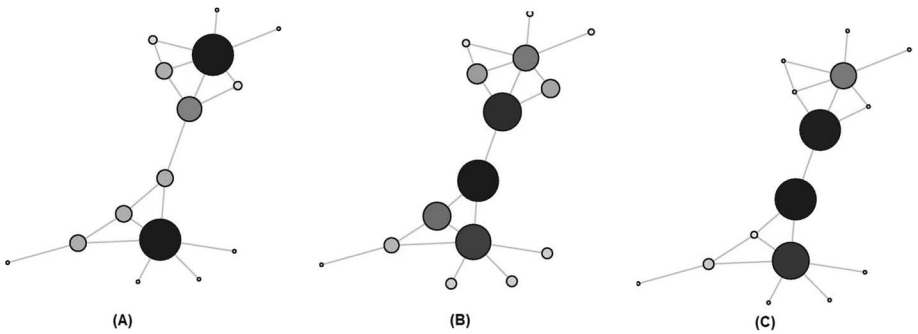

Fig. 1 Network centrality measures. **A** Degree centrality, **B** Closeness centrality, **C** Betweenness centrality. The darkness and the size of each node is proportional to its centrality measure

Here, $\phi^{DC}(i)$ is the weighted degree centrality measure of node i with respect to node j, $e(i,j)$ represents the edge between nodes j and k whose value is 1 if it exists otherwise it is 0 and n_2 is the total number of nodes i.

Weighted closeness centrality

Freeman's (1978) closeness centrality considers a node's importance to be the shortest distance or path or inverse of the sum of the distances between a given node with respect to other nodes in the network. Mathematically, closeness centrality between nodes i and j is calculated by

$$\begin{aligned} C^C(i) &= \frac{n-1}{\sum_{\forall j \& j \neq i} d(i,j)} \\ &= \frac{1}{n(n-1)} \sum_{\forall j \& j \neq i} d(i,j), \end{aligned} \tag{7}$$

where $C^C(i)$ is the closeness centrality, $d(i,j)$ represents the shortest path or distance between node i and j, while n is the total number of nodes in the network. Here we recalculate the distance by first expressing the sum of the shortest distance between nodes i and j with $\delta = \sum_{\forall j \& j \neq i}^{n} d(i,j)$. Therefore, our new closeness centrality measure is calculated using the equality

$$\frac{n-1}{\delta} = \frac{1}{n(n-1)}\delta \tag{8}$$

Rearranging Eq. (8) and taking the positive square root

$$\delta = (n-1)\sqrt{n}, \tag{9}$$

where δ is the shortest distance, $\frac{n-1}{\delta}$ represents closeness centrality based on the shortest distance and $\frac{1}{n(n-1)}\delta$ represents closeness centrality based on the inverse of the sum of the distances and n is total number of nodes in the network. Hence the shortest distance between nodes i and j is $\delta(i,j)$. If we take Eqs. (2) and (9), we can calculate a new closeness weight of node j by

$$w^{CC}(j) = \frac{s(j)\sum_{k=1}^{n_1}\delta(j,k)}{\ln\left(\sum_{k=1}^{n_1}\delta(j,k)\right)}, \tag{10}$$

where $w^{CC}(j)$ is the closeness centrality weight of node j, $\delta(j,k)$ is the shortest distance or path between nodes j and k and n_1 is the total number of nodes k in the network. Of course,

$$\delta(j,k) = \begin{cases} 1 & \text{if the shortest path exists between } i \text{ and } k \\ 0 & \text{otherwise} \end{cases} \tag{11}$$

Therefore, using Eq. (10) we can calculate the weighted closeness centrality score of node i by

$$\phi^{CC}(i) = \sum_{j=1}^{n_2} w^{CC}(j)\delta(i,j), \tag{12}$$

where $\phi^{CC}(i)$ is the weighted closeness centrality measure of node i with respect to node j, $\delta(i,j)$ is the shortest distance or path between nodes j and k whose value is 1 if it exists otherwise it is 0 and n_2 is the total number of nodes j.

Weighted betweenness centrality

Freeman's (1978) betweenness centrality considers that a node's importance is to the number of times that node occurs in the shortest paths between all possible pairs of nodes in a network. Mathematically, betweenness centrality of a node j is calculated by,

$$C^{B}(j) = \sum_{\substack{i=1 \\ i\neq j}} \sum_{\substack{k=1 \\ k\neq j}} \left(\frac{\sigma_{ik}^{*}(j)}{\sigma_{ik}} \right), \tag{13}$$

where σ_{ik} is the total number of shortest paths from node i to node k and $\sigma_{ik}^{*}(j)$ is the number of shortest paths between nodes i and k with node j acting as an intermediate/bridge node along the shortest path. If we use the betweenness value i.e. number of shortest paths between node i and k in Eq. (13), then we provide a new formulation for calculation of the betweenness weight of node j by

$$w^{BC}(j) = \frac{s(j)\sum_{k=1}^{n_1}\sigma_{ik}^{*}(j)}{\ln\left(\sum_{k=1}^{n_1}\sigma_{ik}^{*}(j)\right)}, \tag{14}$$

where $w^{BC}(j)$ is the betweenness centrality weight of node j, $\sigma_{ik}^{*}(j)$ represents the intermediary node between nodes i and j, and n_1 is the total number of node k in the network. Also,

$$\sigma_{ik}^{*}(j) = \begin{cases} 1 & \text{if node } j \text{ exists between } i \text{ and } k \\ 0 & \text{otherwise} \end{cases} \tag{15}$$

Thus, with Eq. (15) we can calculate the weighted betweenness centrality score of node i by

$$\phi^{BC}(i) = \sum_{j=1}^{n_2} w^{BC}(j)\sigma_{jk}^{*}(i), \tag{16}$$

where $\phi^{BC}(i)$ is the weighted betweenness centrality measure of node i, $\sigma_{jk}^{*}(i)$ represents the intermediary node between nodes j and k whose value is 1 if it exists otherwise it is 0 and n_2 is the total number of nodes j.

Application on network pharmacology

Data preparation

Compositive compounds of Ruellia herbs

The chemical compounds of the two *Ruellia* herbs were retrieved from chemistry database (Allen and Motherwell 2002) and PubChem (Kim et al. 2016). From the database, a total of 103 *Ruellia prostrata* and 103 *Ruellia bignoniiflora* active compounds were collected. Using ADMETlab 2.0, an online pharmacokinetics and toxicity prediction program (Xiong et al. 2021), drug-likeness of the active compounds were evaluated. The compounds were subsequently screened for oral bioavailability and drug-likeness by setting filter values at OB $\geq$ 30% (Xu et al. 2012) and DL $\geq$ 0.18 (Clark and Pickett 2000) respectively. This enabled the discovery of the active compounds in *Ruellia* herbs interacting with putative targets proteins (Nickel et al. 2014).

Putative targets for Ruellia herbs

All putative targets related to two *Ruellia* herbs were retrieved from the STITCH database, an online tool for exploring chemical and protein interactions (Kuhn et al. 2007). To obtain the putative targets we restricted the search to "Homo sapiens" and confidence score $>$ 0.4. Only the proteins that directly interacted with *Ruellia* herbs compositive compounds were selected as putative targets. Hence, we collected distinct putative targets related to compositive compounds of the two *Ruellia* herbs.

Known RA therapeutic targets

The known RA therapeutic targets were obtained from three sources those include; First source was DrugBank database (Wishart et al. 2018) (http://www.drugbank.ca, version 4.3),an online tool that provides comprehensive information on drug target data. In this database the search term was restricted to "rheumatoid arthritis" and only FDA approved gene/protein targets linked to rheumatoid arthritis were selected (Mogul et al. 2019). Second source was Online Mendelian Inheritance in Man (OMIM) (Amberger et al. 2019), (http://www.omim.org/), an online tool that cataloged all known diseases and link them relevant genes in human genome. From the database we search for the keyword 'rheumatoid arthritis'. Third source was Therapeutic Target Database (Wang et al. 2020), (TTD, http://db.idrblab.net/ttd/), an online tool that provides information on known and explored therapeutic proteins and nucleic acid targets. The search term was restricted to "rheumatoid arthritis" and only successfully clinically approved therapeutic targets were selected. All the therapeutic targets retrieved from the three source were carefully screened and redundant targets eliminated. A total of 410 important known RA therapeutic were sleeted for the study.

Protein–protein interaction (PPI) data

Eight public database sources were used to retrieved protein–protein interaction data those includes: Online Predicted Human Interaction Database (OPHID) (Brown and Jurisica 2005), Reactome (D'Eustachio 2011), IAct (Kerrien et al. 2012), Human Protein Reference Database (HPRD) (Prasad et al. 2009), Molecular Interaction Database (MINT) (Licata et al. 2012), Database of Interacting Proteins (DIP) (Lehne and Schlitt 2009), PDZBase (Beuming et al. 2005) and STRING (Szklarczyk et al. 2021). We removed all the retardant entries from the eight sources and merged all the data.

Network construction

The herbs, compositive compounds, putative targets and known RA therapeutic targets data were used to perform network construction as follows: (1) herb-compositive compound-putative target network was built by linking the two Ruellia herbs, compositive compounds and corresponding putative targets; (2) herb-putative target-known RA therapeutic target network was established by linking the two Ruellia herbs, corresponding putative targets, and known RA therapeutic target that interacted with putative targets; and (3) imbalance multi-level network was built by linking herb-compositive compound-putative targets and herb-putative targets-known RA therapeutic targets-other human PPI network built by linking herb-compositive compounds-putative targets network and herb-putative target-known RA therapeutic target-Other human protein's PPI network directly interacting with the two targets. The nodes with high weighted centrality score i.e. "Degree centrality", "Closeness centrality", "Betweenness centrality" were considered as important nodes in the network.

Gene ontology enrichment and KEGG pathway analysis

To perform the Gene Ontology (GO) enrichment and KEGG pathway analysis, DAVID database (https://david.ncifcrf.gov) (Dennis et al. 2003; Aoki and Kanehisa 2005) were used. To obtain enriched GO terms, functional categories including biological processes and molecular functions were evaluated for the major common putative targets. KEGG pathways analysis was also performed to establish the pathway mechanism of the major common putative targets.

Molecular docking simulation

Molecular docking is a in silico method widely used in drug discovery and design to investigate the inter-molecular interaction and prediction of the binding affinity and conformation (Agarwal and Mehrotra 2016). In this study, AutoDock version 4.2.6 was utilised to perform docking simulation (Cosconati et al. 2010; Morris et al. 2008). The binding affinity was the calculated based on the semi-empirical free energy force field scoring function (Huey et al. 2007) given by equation below

$$\begin{aligned}\triangle G = &\left(V_{bond}^{L-L} - V_{unbond}^{L-L}\right) + \left(V_{bond}^{P-P} - V_{unbond}^{P-P}\right) \\ &+ \left(V_{bond}^{P-L} - V_{unbond}^{P-L} + \triangle S_{conf}\right)\end{aligned}$$

where $\triangle S_{conf}$ denotes conformation entropy lost during binding, L and P denotes the ligand and protein respectively.

The candidate compounds (ligands) and proteins (receptors) for docking analysis were selected based on the weighted centrality score value calculated from the imbalance multi-level network analysis results. Hydroxychloroquine (Fox 1993) and Methotrexate (Kremer et al. 1994) were chosen as positive control drugs in the treatment of rheumatoid arthritis. The chemical structures of the candidate compounds were obtained in SDF file format from PubChem (Kim et al. 2016) while the crystal structure of the target proteins were retrieved from RCSB database (Deshpande et al. 2005). Open Babel tool

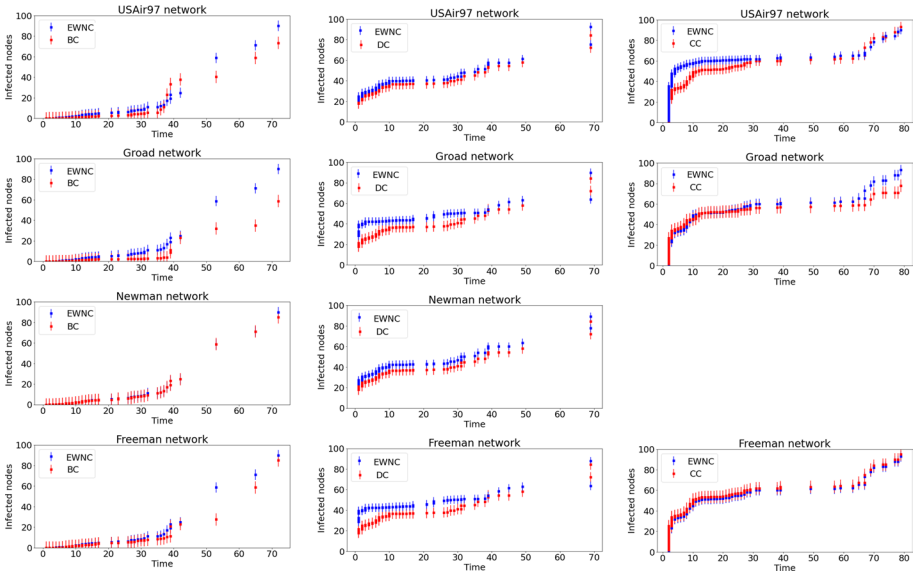

Fig. 2 The comparison of EWNC with other classical centrality measures in real networks. The real network data are obtained from USAir97 network, Groad network, Newman network and Freeman's network. The figures show comparison of the cumulative number of infected nodes as function of time-step

(version 2.4.1, http://openbabel.org) (O'Boyle et al. 2011) was utilised to convert compounds to PDB file format. AutoDockTools was utilised to import the Candidate ligands and receptors, which were then subjected to the following prepossessing steps: (1) elimination of the all hetero-atoms and water molecules; (2) addition of the polar hydrogens with Gasteiger and Kollman charges to ligands and receptors receptively and (3) conversation of output file into pdbqt. file format. The docking search area was calculated based on (Feinstein and Brylinski 2015), we set grid box dimension of $60 \times 60 \times 60$ Å with a spacing of 0.479 Å for optimal docking results. The 2D and 3D interaction of hydrogen atoms and amino acid residues were visualised using LigPlot+ versions 2.2 (Laskowski and Swindells 2011) and PyMol2.5 (DeLano et al. 2002) software's respectively.

Results

Evaluation of EWNC performance

The performance of our proposed EWNC was evaluated using four real network data obtained from Freeman's electronic information exchange system (EIES) network (Iacobucci et al. 2017), USAir97 network (Zhao et al. 2020; Fei et al. 2017), Groad network (Wang et al. 2017; Zhao et al. 2020), and Newman's scientific collaboration network (Newman 2001, 2001). We adopt the Susceptible-Infected (SI) Model (Zhou et al. 2006) to assess the spreading influence of the top-L ranked nodes from the networks based on our EWNC method and other existing weighted centrality measures. In this analysis we denote weights of degree centrality (DC),betweenness centrality (BC) and closeness centrality (CC) of the existing centrality measures by DC_w, BC_w and CC_w respectively. To evaluate the performance we compared the cumulative number of infected nodes with the initial nodes appearing at the top of the list for different centrality measures. Figure 2 show the comparison results of our EWNC method and other existing centrality measures applied in the four real networks data.

In USAir97 network data, it can be seen that final number of infected nodes for our EWNC approach is higher compared to other centrality measures. In addition, we can note that our approach outperforms other method in the calculation of DC_w and BC_w. Though after time step 30 the node spread is nearly the identical to CC_w, the propagation speed of our proposed EWNC at early stage is rapid. Also it can be observed that our EWNC has minimal error indicating that the method is more effective and accurate in calculation of the influential nodes in the network. In the Groad network, the difference in performance between our EWNC approach and other centrality measures can be noted in DC_w and BC_w which indicate an increase in number of infected nodes after time-step $t \geq 30$. When $t \leq 30$, the infection process with CC_w is nearly identical, and the errors of EWNC are clearly smaller than those of DC_w and BC_w. In the Newman's network, we observed that when $t = 20$, EWNC achieves nearly the same performance of infected nodes as DC_w. When t is between 20 and 50, EWNC outperforms BC_w for spreading ability and has better infection effect and less error than BC_w. The performance of EWNC is slightly identical to DC_w. In Freeman's network, EWNC outperforms both DC_w and BC_w. We noted that our EWNC approach also behaves similarly to or close to CC_w, however, with minimal error when when compared to DC_w, BC_w, and CC_w. This means that our proposed EWNC calculation is more precise. Generally, this analysis confirms our EWNC approach to be robust and efficient in the identification of the influential node in the real complex networks. This provides prospect of its application in solving other complex network problems.

Network pharmacology simulation

Herb-compositive compound-putative target network analysis

To establish the relationship between the two *Ruellia* herbs and putative targets we built the herb-compositive compound-putative target network as shown in Fig. 3, which includes 634 nodes (2 herbs, 196 compositive compounds, and 436 putative target genes) and 5212 edges. According to the network analysis, all the *Ruellia* compositive compounds interacted with 436 putative target. Markov cluster (MCL) analysis of the network indicate that from a total of 196 compositive compounds identified from the network, 103 compounds originated from *Ruellia prostrata* herb and 93 compounds came from *Ruellia bignoniiflora* herb. Further cluster (MCL) analysis to extract and identify compositive compounds common in both *Ruellia* herb. According to results in Fig. 4, 22 compositive compounds were common to both *Ruellia* herbs and had high centrality scores values indicating their importance in the network. For instance high centrality score values of putative targets including CSF2, CXCL1, CCL2, CCR2 and TNF indicated interaction with multiple common compositive compounds such as Glyceryl-2 Palmitate, Glycidyl oleate, Oleoyl chloride, Glyceryl diacetate-2-Oleate and Hexadecanoic acid, methyl ester. This network provided clue on relationship between *Ruellia* compositive compounds and corresponding putative targets.

Compositive compound-putative target-RA known target network analysis

To establish the relationship between compositive compounds, the putative targets and the known RA therapeutic targets, compositive compound-putative target-known RA

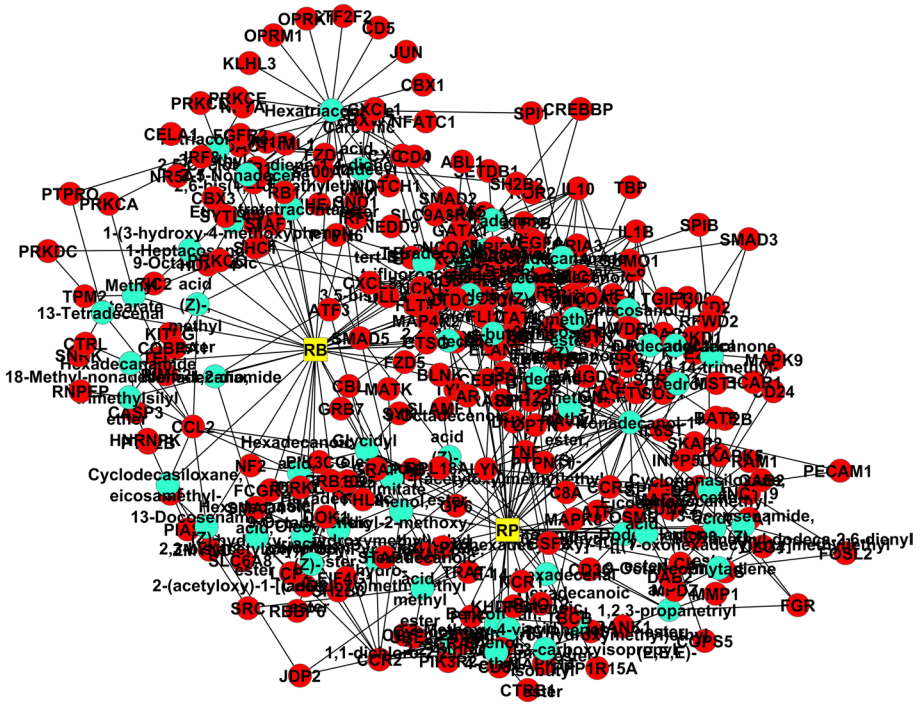

Fig. 3 Herb-compositive compound-putative target network. Edges: interactions between herbs, compounds and putative target; yellow square nodes: *Ruellia prostrata* (RP) and *Ruellia bignoniiflora* (RB) herbs; green round nodes: RP–RB compositive compounds; red round nodes: putative targets

therapeutic target network shown in Fig. 5 was built. The network composed of 1042 nodes (196 compositive compounds, 436 putative target and 410 known RA therapeutic targets) and 6964 edges. Based on the network analysis six known RA therapeutic targets including Delta-type opioid receptor, Nitric oxide synthase, Prostaglandin G/H synthase 1, Cannabinoid receptor 2, Prostaglandin G/H synthase 2 and Tumor necrosis factor showed high degree centrality score values a clear indication of interaction with multiple corresponding compositive compounds and putative targets in the network. Putative targets including TNF, IL6, FOXP3, CSF2, CCR2, CCR5 and CSF2 as well as 8 compositive compounds including Glycidyl oleate and Glyceryl-2 Palmitate, Oleoyl chloride, 9-Octadecenoic acid (Z)-, methyl ester, Methyl stearate, Hexadecanoic acid, methyl ester, Hexadecanoic acid, 2,3-bis(acetyloxy)propyl ester and Glyceryl diacetate-2-Oleate indicated highest centrality score values in the network. This network provided an insight on relationship between *Ruellia* compositive compounds and the corresponding putative targets and know RA therapeutic targets.

Imbalance multi-level network analysis

To understand the mechanism of action of two *Ruellia* herbs in the treatment of rheumatoid arthritis an imbalance multi-level network consisting of herb-compositive compound-putative targets-known RA therapeutic targets-PPI network was built by merging herb-compositive compounds-putative targets network as shown in Fig. 2, compositive compound-putative target-known RA therapeutic target network as shown in Fig. 3 and herb-putative target-known RA therapeutic target-Other human protein's

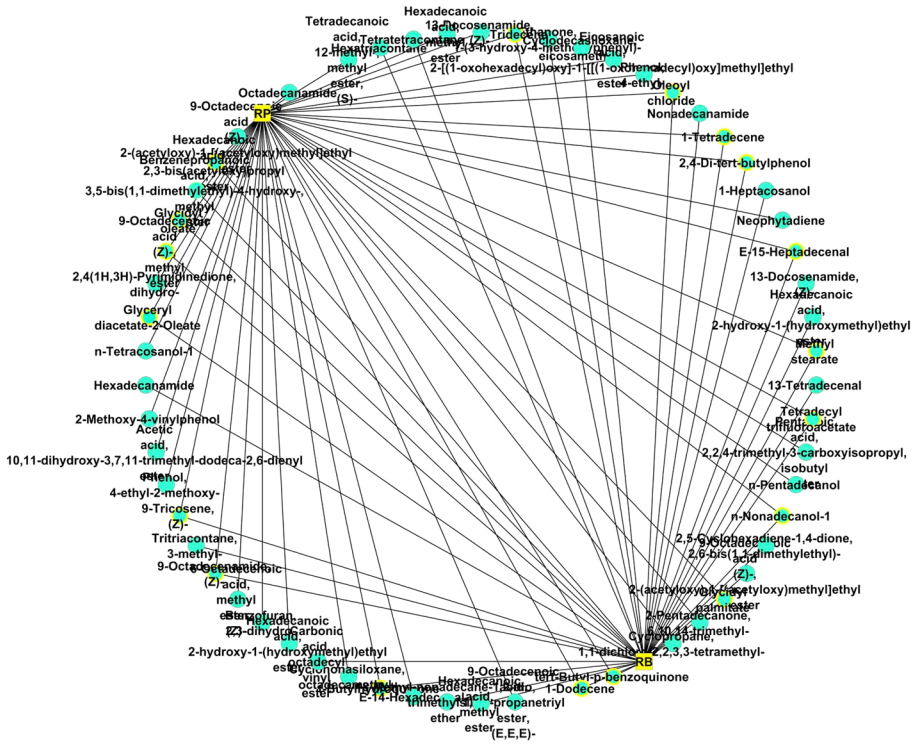

Fig. 4 Herb-compositive compound network. Edges: interactions between herb and compositive compounds; yellow square nodes: *Ruellia prostrata* (RP) and *Ruellia bignoniiflora* (RB) herbs; green round nodes: RP–RB compositive compounds; green nodes with yellow border are compounds shared by the two *Ruellia* herbs

PPI network as shown in Fig. 6A. Figure 6B show an imbalance multi-level network composed of 1519 nodes (2 herbs, 196 compositive compounds, 436 putative targets, 410 known RA therapeutic targets and 475 other human proteins interacting with putative targets or known RA therapeutic targets) and 9375 edges. The significant network components were then identified based on weighted centrality score values. Network analysis revealed a total of 57 nodes (2 herbs, 8 compositive compounds, 15 putative targets, 10 known RA therapeutic targets and 24 other human proteins interacting with putative targets or known RA therapeutic targets) and 417 edges with high centrality score values ('Degree centrality', 'Betweenness centrality' and 'Closeness centrality') indicating their significance in the network as shown in Table 1. From the network Glycidyl oleate, Glyceryl-2 Palmitate, Oleoyl chloride, 9-Octadecenoic acid (Z)-, methyl ester, Methyl stearate, Hexadecanoic acid, methyl ester, Hexadecanoic acid, 2,3-bis(acetyloxy) propyl ester and Glyceryl diacetate-2-Oleate compounds indicated high interaction with the corresponding putative targets, known RA therapeutic targets and other human proteins. This network provided clue on the relationship between *Ruellia* herbs, compositive compounds, putative targets, know RA therapeutic targets and other human protein which explains the mechanism of action of the *Ruellia* herbs in the treatment of rheumatoid arthritis (Fig. 6A and B).

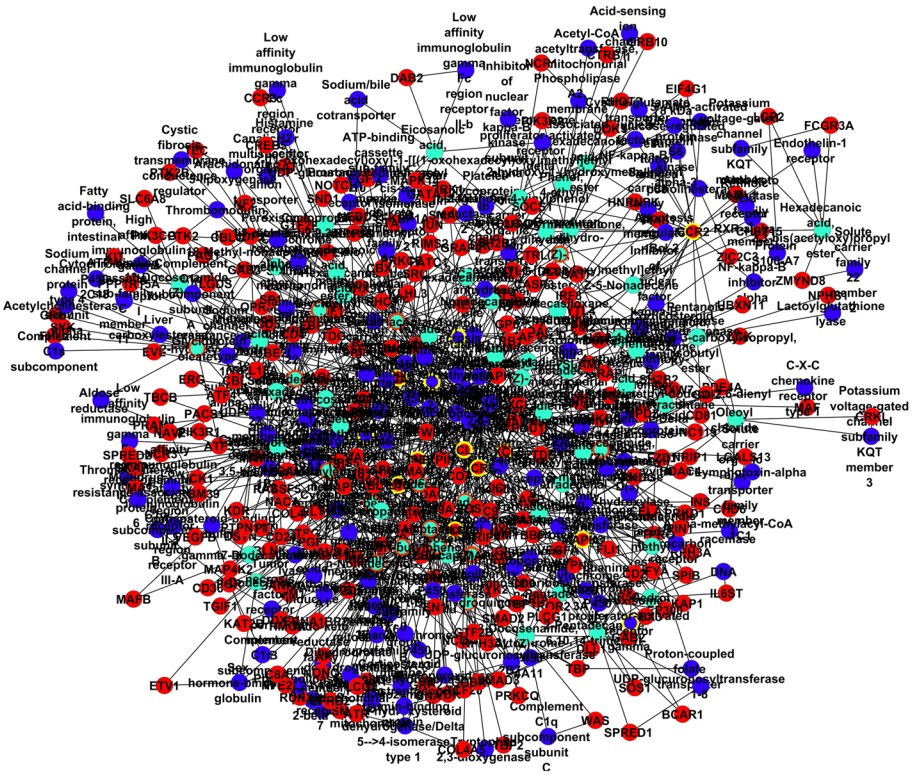

Fig. 5 Compositive compound-putative target-RA known target network. Edges: interactions among compositive compounds, putative targets and known RA therapeutic targets. Green round nodes: RP–RB compositive compounds; red round nodes: putative targets; blue round nodes: RA known therapeutic targets. Nodes with yellow are major components with corresponding high weighted centrality scores.

Gene ontology and pathway enrichment analysis

A total of 39 major targets (15 putative targets and 24 other human proteins) of *Ruellia* herbs related to rheumatoid arthritis obtained from the imbalance multi-level network were utilised to perform Gene Ontology and Pathway enrichment analysis. Figure 7 show a summary of the significant biological process, molecular function and top-10 KEGG pathway associated with associated with rheumatoid arthritis. According to the analysis top-18 enriched GO terms for biological process Fig. 7A and molecular function Fig. 7B included the were Cytokine-mediated signaling pathway, Inflammatory response, Intracellular signal transduction, Regulation of cell population proliferation, Cytokine receptor binding, Chemokine receptor binding, CXCR chemokine receptor binding,CCR2 chemokine receptor binding and CXCR chemokine receptor binding. In addition, we perform KEGG pathway analysis for the major targets and the top-10 enriched pathways were were IL-17 signaling,IL-10 signaling, TNF signaling, IL-4 and IL-13 signaling, Toll-like receptor signaling signaling pathway, NF-kappa B signaling, CCR interaction, NOD-like receptor signaling pathway, Chemokine signaling pathway, and GPCR ligand binding. The IL-17 signaling pathway promotes neutrophil mobility via T cell activation, which help against inflammatory illnesses such as rheumatoid arthritis (Raucci et al. 2022). TNF signaling is a multifunctional cytokine and plays an important role in pro-inflammatory cytokine (Chen et al. 2022). NF-kappa B signaling pathway

Table 1 Weighted centrality scores of major targets acting on rheumatoid arthritis

Compositive compounds	ϕ^{DC}	ϕ^{BC}	ϕ^{CC}
Glycidyl oleate	0.5342	0.0485	0.5581
Glyceryl-2 palmitate	0.5109	0.0517	0.5892
Oleoyl chloride	0.4589	0.0528	0.4706
9-Octadecenoic acid (Z)-, methyl ester	0.4316	0.0525	0.4752
Methyl stearate	0.4446	0.0489	0.4468
Hexadecanoic acid, methyl ester	0.4472	0.0532	0.4656
Hexadecanoic acid, 2,3-bis(acetyloxy)propyl ester	0.4912	0.1413	0.4842
Glyceryl diacetate-2-Oleate	0.4509	0.0517	0.4892
Known RA targets			
Nitric oxide synthase	0.4982	0.0565	0.5681
Interleukin-1β	0.4106	0.0493	0.4855
Delta-type opioid receptor	0.5417	0.1199	0.4944
Tumor necrosis factor	0.4626	0.1696	0.4896
Prostaglandin G/H synthase 2	0.4933	0.3967	0.5411
Prostaglandin G/H synthase 1	0.4551	0.5040	0.4794
Growth-regulated alpha protein	0.4126	0.0888	0.5249
C–C chemokine receptor type 5	0.4026	0.0589	0.4609
Interleukin-6	0.4244	0.0671	0.5158
Cannabinoid receptor 2	0.4700	0.0401	0.4352
Putative targets			
TNF	0.2705	0.0921	0.0588
CXCL10	0.1728	0.0116	0.5640
IL10	0.1728	0.0125	0.5433
IL6	0.3004	0.0930	0.5402
CXCL1	0.1044	0.0151	0.5432
CXCL8	0.1273	0.0160	0.5439
FOXP3	0.4106	0.0149	0.3748
CCR2	0.3004	0.0161	0.4762
CCR5	0.3004	0.0279	0.4922
IL10	0.1273	0.0145	0.5302
CCL2	0.2495	0.0190	0.4548
IL1B	0.1405	0.0253	0.5838
IL17	0.2495	0.0195	0.5374
IL13	0.2212	0.0252	0.5347
CSF2	0.2905	0.0996	0.5101

play important role in inflammatory and immunological responses, as well as regulating genes involved in cell death, differentiation, and proliferation (Cao et al. 2022). Furthermore, the modulation of chronic inflammatory synovitis by cytokines has been linked in

(See figure on next page.)

Fig. 6 Herb-compositive compound-putative target-RA known target-PPI network. **A** Herb-putative target-RA known targets network; **B** Imbalance multi-level network of herb-compositive compound-putative target-RA known target-PPI network. Edges: interactions among the two herbs, compositive compounds, putative targets, RA known therapeutic targets and Other Human proteins' PPI Network. Yellow square nodes: *Ruellia prostrata* (RP) and *Ruellia bignoniiflora* (RB) herbs; green round nodes: RP–RB compositive compounds; red round nodes: putative targets; blue round nodes: RA known therapeutic targets; purple round nodes: Other Human proteins. Nodes with yellow borders are major components with corresponding high weighted centrality scores

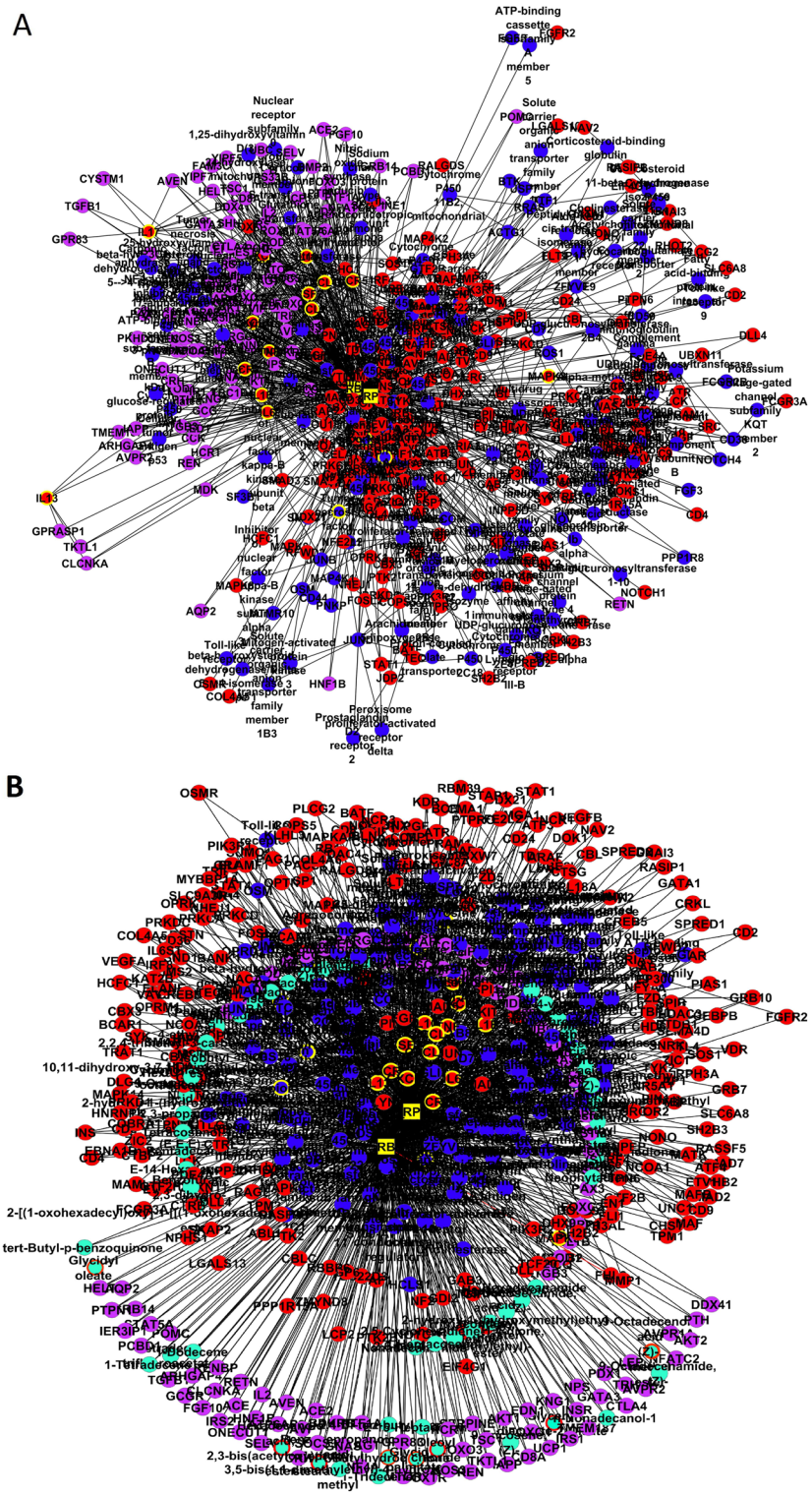

Fig. 6 (See legend on previous page.)

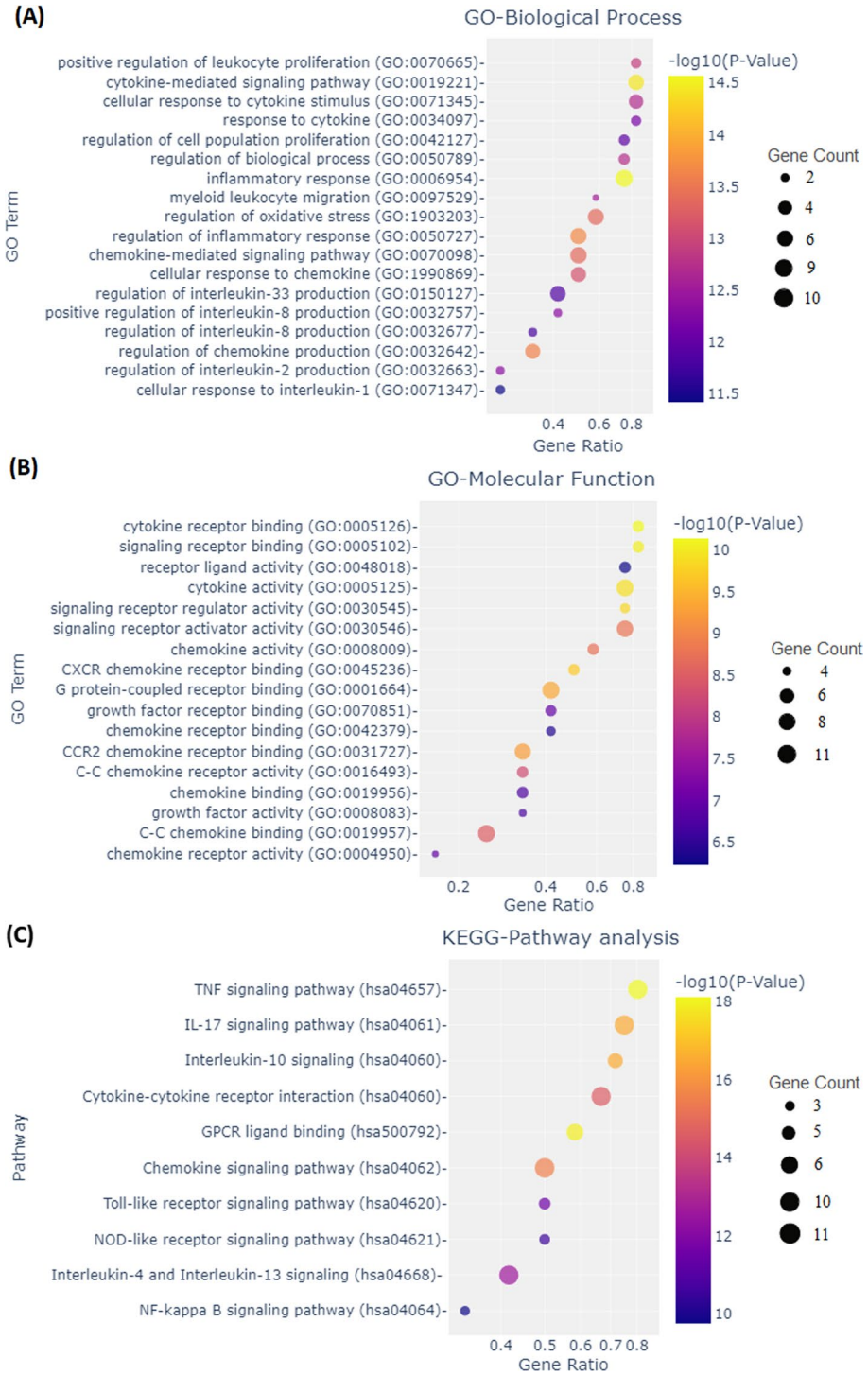

Fig. 7 GO enrichment and KEGG pathway analysis for major putative targets. **A** Biological process; **B** Molecular function; and **C** Top 10 KEGG pathway. KEGG, Kyoto Encyclopedia of Genes and Genomes

several cases of rheumatoid arthritis (Skrzypkowska et al. 2022). IL-1 and TNF are the main pro-inflammatory cytokines in rheumatoid arthritis may play an important role in rheumatoid arthritis management (Koper-Lenkiewicz et al. 2022). NOD-like receptor signaling pathway are involved in tissue injury and infection by activating the synthesis of pro-inflammatory cytokine receptors Weyand and Goronzy (2021). TLRs and NOD-like receptors have been linked to inflammatory joint disease (Swain et al. 2022). Chemokines have been linked to a variety of neurological illnesses, mainly via generating inflammation through the chemotactic localization of leukocytes (Skrzypkowska et al. 2022). Chemokine activities mediated by G-protein coupled receptors, play an role in inflammatory reactions (Cheng et al. 2022). Interleukin-10, Interleukin-4 and Interleukin-1β signaling pathways have been implicated in the regulation of the type II inflammatory and anti-inflammatory cytokine which plays a critical role in the regulation of inflammatory processes (de Freitas et al. 2022; Bridgewood et al. 2022).

Molecular docking evaluation

In the compound-target network, the top eight compositive compounds (Glyceryl diacetate-2-Oleate, Glyceryl-2 Palmitate, Hexadecanoic acid, 2,3-bis(acetyloxy)propyl ester, Methyl stearate, Glycidyl oleate, Oleoyl chloride, Hexadecanoic acid, methyl ester, and 9-Octadecenoic acid (Z)-, methyl ester) and the top nine targets (TNF, NOSs, IL-1β, PTGS2, IL-6, PTGS2,DOP, CCR5 and CB2) were selected and molecular docking evaluation was performed. In Table 2 we present top-4 compounds with best binding energy and Lipinski Properties. According to the results, Glyceryl diacetate-2-Oleate and Oleoyl chloride indicated a HIGH binding energy with all target proteins. Though Glyceryl diacetate-2-Oleate had the highest binding energy against TNF (−10.33 kcal/mol) and

Table 2 Molecular docking and Lipinski properties of the major compositive compounds

Target receptors	Cp1		Cp3		Cp5		Cp6	
	B.E (kcal/mol)	RMSD	B.E (kcal/mol)	RMSD	B.E (kcal/mol)	RMSD	B.E (kcal/mol)	RMSD
TNF	− 10.33	1.212	− 9.98	1.921	− 9.96	1.774	− 9.31	1.605
NOSs	− 8.91	2.163	− 8.72	2.269	− 8.31	2.123	− 9.25	1.664
IL-1β	− 8.82	2.311	− 8.73	2.129	− 8.71	2.391	− 8.45	2.111
DOP	− 8.45	2.121	− 9.16	1.218	− 9.43	1.627	− 8.37	2.011
PTGS2	− 9.87	1.411	− 9.65	1.632	− 9.71	1.613	− 9.38	1.494
PTGS1	− 9.98	1.721	− 9.83	1.575	− 8.38	2.176	− 8.09	2.278
IL-6	− 9.82	1.263	− 8.81	2.163	− 8.61	2.037	− 8.42	2.126
CCR5	− 10.52	1.019	− 10.32	1.135	− 9.52	1.147	− 10.02	1.201
CB 2	− 9.06	1.847	− 8.35	2.378	− 8.96	2.041	− 8.11	2.263
Lipinski properties								
LogP	8.02		7.5		7.72		8.6	
H-donor	0		0		0		0	
H-acceptor	6		6		3		1	
nrotb	23		22		18		15	
TPSA	78.92		78.92		38.83		17.07	
MW	440.31		414.30		338.61		300.22	

Cp1: Glyceryl diacetate-2-Oleate; Cp3: hexadecanoic acid, 2,3-bis(acetyloxy)propyl ester; Cp5: glycidyl oleate; Cp6: oleoyl chloride; logP: molecular lipophilicity potential; nrotb: number of rotatable bond; TPSA: topological polar surface area; MW: molecular weight

CCR5 (−10.52 kcal/mol). Hexadecanoic acid, methyl ester recorded low binding energy for all other the target proteins except against TNF and L−1β. Compound or ligands with binding energy within the range of −8.0 kcal/mol and −11.0 kcal/mol as well as RMSD $\leq$ 2.5 Å is clear indication of a good molecular interaction between the compounds and the target receptors.

We evaluate the drug-likeliness of the candidate drug compounds using Molinspiration an online software (Molinspiration 2011) for prediction of molecular properties. We applied Lipinski rule of five which state that "drug-like" molecules have logP$\leq$ 5, molecular weight $\leq$ 500, hydrogen bond acceptors $\leq$ 10 and hydrogen bond donors $\leq$ 5 (Zhang and Wilkinson 2007; Chen et al. 2020). The results in Table 2 indicate that the all four candidate drug compounds were within the limits of Lipinski's rule. Also we evaluated the Topological Polar Surface Area (TPSA) (Ertl et al. 2000) to predict the candidate drug compounds permeability. The result indicated that all the compounds had the TPSA in within the set limit of $\leq$ 140 Å^2. A clear indication of compounds good drug absorption properties such bioavailability, intestinal absorption, Caco-2 permeability, and blood-brain barrier penetration (Francis and Chakraborty 2022; Ertl et al. 2000). In addition, the number of rotatable bond were within the established limit of 6–170 rotatable bonds (Hamri et al. 2022). A high number of rotatable bonds indicates high molecular flexibility, which acts as an indicator of a good oral bioavailability of the drugs (Veber et al. 2002).

To illustrate the surface interaction and conformation between the candidate compound and the target proteins, it was necessary to visualise the 3D conformations of the andidate compound and the target proteins using Pymol software. Figure 8, show the 3D surface interaction of the Glyceryl diacetate-2-Oleate against selected major target receptors (TNF, NOSs, IL-1β, PTGS1, IL-6, PTGS2,DOP, CCR5 and CB2. We can observe that Glyceryl diacetate-2-Oleate had high hydrogen bond interactions with side chain amino acid and and a slight hydrophobic interaction with the targets proteins.

We also, illustrate the surface interaction and conformation between the Oleoyl chloride (cp6) against the six selected major target receptors (TNF, NOSs, IL-1β, PTGS1, IL-6, PTGS2,DOP, CCR5 and CB2. Again, in Fig. 9 we observe that Oleoyl chloride had high hydrogen bond interactions with side chain amino acid and sa slight hydrophobic interaction with the targets proteins.

In drug design, it is critical to understand the interaction of the hydrogen bond of the drug compounds and amino residue of target proteins or receptors. In this study we evaluated the interaction of the hydrogen bonds of the ligand and amino residues of the target protein and visualise 2D interaction using the LigPlot+ Software. Figure 10 show the interaction of the hydrogen bond in Glyceryl diacetate-2-Oleate (cp1) against amino residues of six selected major target proteins (TNF, NOSs, IL-1β, PTGS1, IL-6, PTGS2,DOP, CCR5 and CB2). We can observe that the CB2 and Glyceryl diacetate-2-Oleate had interaction of two hydrogen bonds with Trp1060, and Asp1095. IL-1β with Glyceryl diacetate-2-Oleate formed hydrogen bond interaction with Asn130 and Asn132. IL-6 and Glyceryl diacetate-2-Oleate formed hydrogen bond interaction with Thr156 and Thr161 amino acid residues. PTGS1 with Glyceryl diacetate-2-Oleate formed hydrogen bond interaction with Ser530. TNF with Glyceryl diacetate-2-Oleate

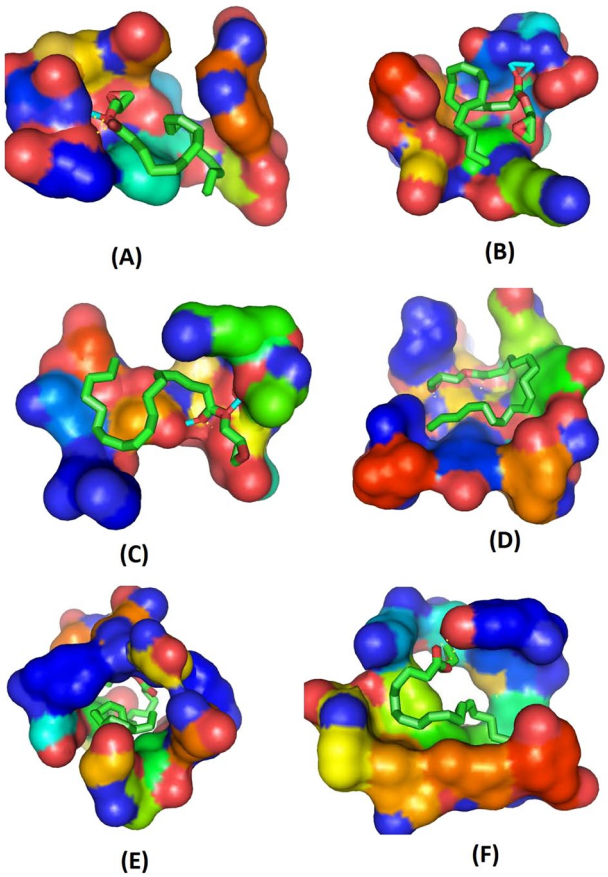

Fig. 8 3D surface interaction and conformation between Glyceryl diacetate-2-Oleate (Cp1) and six selected targets of *Ruellia* herbs. **A** Cp1 and CB2; **B** Cp1 and IL-1β; **C** Cp1 and IL-6; **D** Cp1 and TNF; **E** Cp1 and PTGS1; **F** Cp1 and DOPR. The blue colour indicates hydrogen bond interactions with side chain amino acid (mild polar) and pink represents the hydrophobic interactions

formed hydrogen bond interaction with Try151 amino acid residue. DOP with Glyceryl diacetate-2-Oleate had hydrogen bond with Ser100 amino acid residue.

Similarly, we evaluated the interaction of the hydrogen bond in Oleoyl chloride (cp6) against and amino residues of six selected target proteins. From Fig. 11, We observed that CB2 and Oleoyl chloride had three hydrogen bonds with Asn1014, Thr1012 and Gly1013. IL-1β with Oleoyl chloride had hydrogen bonds with Arg102 and His298. IL-6 and Oleoyl chloride formed hydrogen bonds with Ala143, Asn191 and Asn171 amino acid residues. PTGS1 and Oleoyl chloride had hydrogen bond interaction with Ser530. PTGS2 and Oleoyl chloride had hydrogen bond interaction with Trp385. NOSs and Oleoyl chloride had hydrogen bond interaction with Gly371. CCR5 and Oleoyl chloride had hydrogen bond interaction with Thr284. TNF with Oleoyl chloride had hydrogen bonds interaction with Try151 and Gly121. DOP with Glyceryl diacetate-2-Oleate had hydrogen bond interaction with Leu119 and Glu118 amino acid residues.

In our study it was important to evaluate the ADMET properties of the candidate drug compound identified by our proposed weighed network centrality measure and molecular docking simulations. In our scenario we opted to evaluate the absorption, metabolism and toxicity of candidate compounds which play a key role to establish safety of a

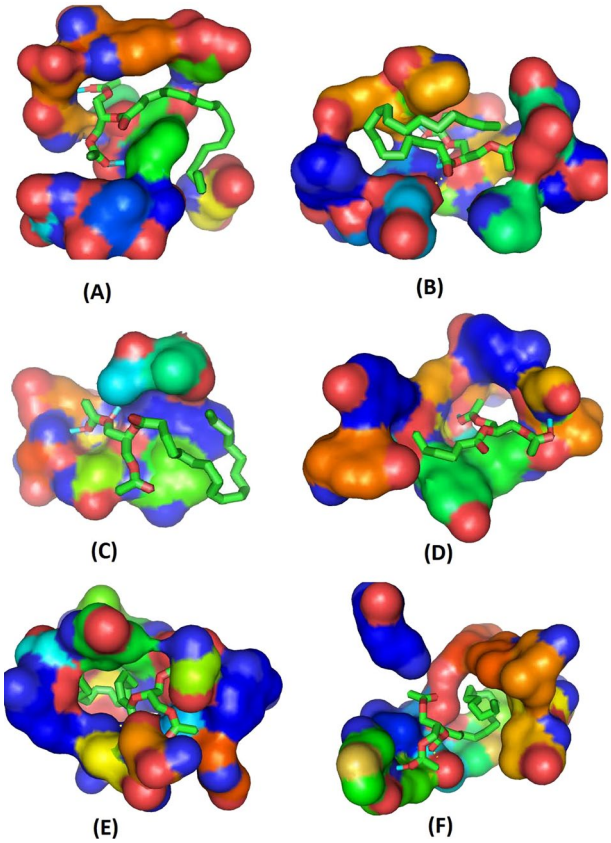

Fig. 9 3D surface interaction and conformation between Oleoyl chloride (Cp6) against six selected target proteins of *Ruellia* herbs. **A** Cp6 and CB2; **B** Cp6 and IL-1β; **C** Cp6 and IL-6; **D** Cp6 and TNF; **E** Cp6 and PTGS1; **F** Cp6 and DOPR. The blue colour indicates hydrogen bond interactions with side chain amino acid (mild polar) and pink represents the hydrophobic interactions

drug compounds. We import the SMILES chemical structure of the four candidate drug compounds into the ADMETlab 2.0 (Dong et al. 2018), an online software for evaluation and screening the pharmacokinetics and toxicity properties of chemical compounds. According the results in Table 3, all the four candidate drug compounds were within the optimal values for Caco-2 Permeability (≥ -5.15) and acted as Non-inhibitor and Non-substrate for Pgp. We also observed that cp1 and cp6 had higher HIA value a clear indication of their high absorption to the gastrointestinal system into the bloodstream. Evaluation of metabolism activity indicates cp3, and cp5 high probability of acting as inhibitor of the metabolic enzyme CYP3A4. while cp3, cp5 and cp6 have high probability of acting as substrate to metabolic enzyme CYP2C9. Evaluation of toxicity properties of the candidate drug compounds show that low probability of hERG Blockers indicating low cardiotoxicity that may results to fatal ventricular arrhythmias and sudden death. All the candidate drug compounds were negative to Human Hepatotoxicity (H-HT). Cp3 recorded significantly higher Drug Induced Liver Injury (DILI $= 0.063$) compared to other drug compounds. we also observed that Cp5 had high AMES Toxicity value a clear indication of mutagenic characteristic and therefore may act as a carcinogen. In addition, all the drug compounds are non-carcinogencity and low Rat Oral Acute Toxicity.

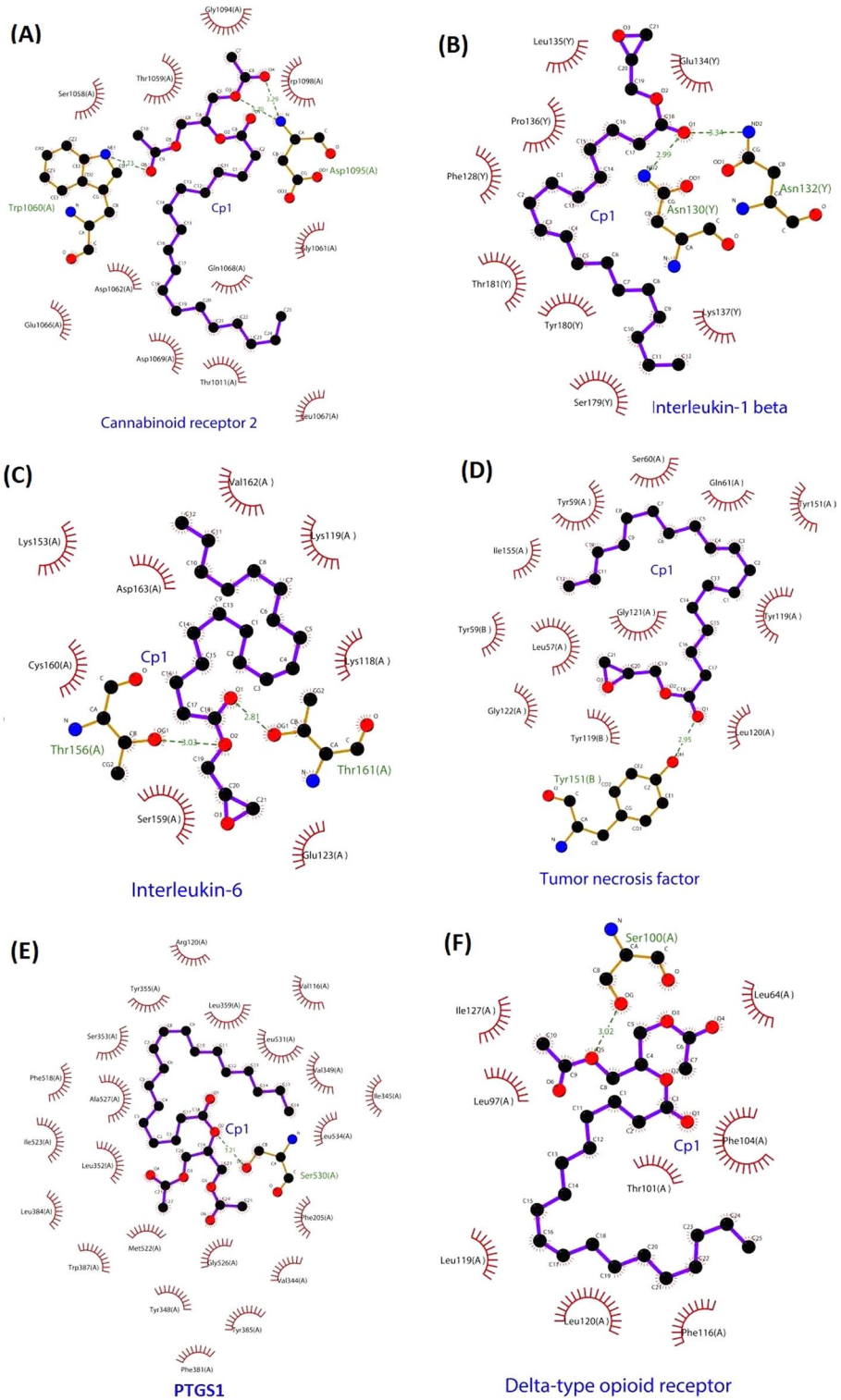

Fig. 10 2D interaction of the hydrogen bond in Glyceryl diacetate-2-Oleate (cp1) against six selected major target proteins of *Ruellia*. **A** Cp1 and CB2; **B** Cp1 and IL-1β; **C** Cp1 and IL-6; **D** Cp1 and TNF; **E** Cp1 and PTGS1; **F** Cp1 and DOPR. The blue colour indicates hydrogen bond interactions with side chain amino acid (mild polar) and pink represents the hydrophobic interactions

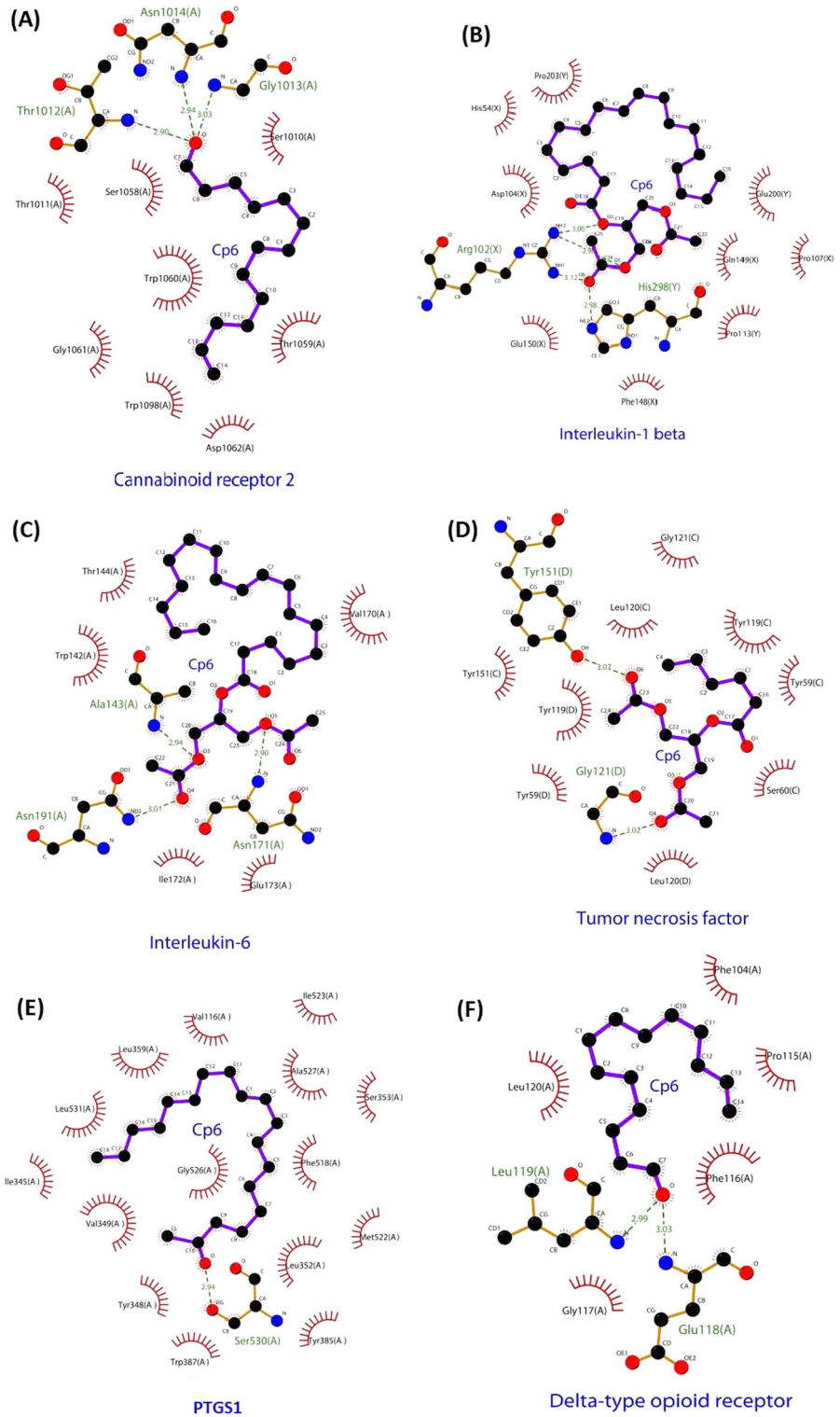

Fig. 11 2D interaction of the hydrogen bond in Oleoyl chloride (Cp6) and six selected target proteins of *Ruellia* herbs. The dashed green lines indicate hydrogen bond and its length; brown line indicates non-ligand bond; purple lines indicate the ligand bonds; red-eyelash symbol with dashed red line indicate non-ligand residue involved in hydrophobic interaction; black dots with dashed red line indicate corresponding atoms involved in hydrophobic interaction(s)

Table 3 ADMET prediction of Absorption, Metabolism and Toxicity of the four candidate drug compounds

	Cp1	Cp3	Cp5	Cp6
Absorption				
Caco-2 permeability	− 4.727	− 4.823	− 4.859	− 4.672
Pgp-inhibitor	0.64 Non-inhibitor	0.959 Non-inhibitor	0.007 Non-inhibitor	0.000 Non-inhibitor
Pgp-substrate	0.003 Non-substrate	0.002 Non-substrate	0.001	0.001 Non-substrate
HIA	0.719*	0.513	0.351	0.815*
Metabolism				
CYP1A2 inhibitor	0.206 Non-inhibitor	0.219 Non-inhibitor	0.245 Non-inhibitor	0.508 Non-inhibitor
CYP1A2 substrate	0.089 Non-substrate	0.100 Non-substrate	0.239 Non-substrate	0.187 Non-substrate
CYP2C19 inhibitor	0.395 Non-inhibitor	0.060	0.326 Non-inhibitor	0.454 Non-inhibitor
CYP2C19 substrate	0.056 Non-substrate	0.178 Non-substrate	0.063 Non-substrate	0.059 Non-substrate
CYP2C9inhibitor	0.311 Non-inhibitor	0.459 Non-inhibitor	0.159 Non-inhibitor	0.291 Non-inhibitor
CYP2C9 substrate	0.248 Non-substrate	0.712 Substrate	0.752 Substrate	0.965 Substrate
CYP3A4 inhibitor	0.487 Non-inhibitor	0.699 Inhibitor	0.633 Inhibitor	0.321 Non-inhibitor
CYP3A4substrate	0.147 Non-substrate	0.162 Non-substrate	0.103 Non-substrate	0.05 Non-substrate
Toxicity				
hERG blockers	0.194	0.292	0.349	0.142
H-HT	0.052 Negative (−)	0.029 Negative (−)	0.082 Negative (−)	0.052 Negative (−)
DILI	0.022	0.063	0.047	0.022
AMES toxicity	0.027 Negative (−)	0.038 Negative (−)	0.796 Negative (−)	0.019 Negative (−)
Rat oral acute toxicity	0.035 Low-toxicity	0.052 Low-toxicity	0.061 Low-toxicity;	0.026 Low-toxicity
Carcinogencity	0.016 Non-carcinogens	0.0596 Non-carcinogens	0.0446 Non-carcinogens	0.012 Non-carcinogens

Cp: Glyceryl diacetate-2-Oleate; Cp3: hexadecanoic acid, 2,3-bis(acetyloxy)propyl ester; Cp5: glycidyl oleate; Cp6: oleoyl chloride; HIA: human intestinal absorption; H-HT: human hepatotoxicity; DILI: drug induced liver injury

Discussion

Comparison EWNC to other centrality measures

This study proposed an new efficient weighted network centrality measure by modification classical centrality using node interconnectivity score which consider interaction between pair of nodes and number shared neighborhood in the network. According to simulation results in Fig. 2, SI model was used to evaluate the node spreading process (cumulative number of infected nodes) in four real networks by comparing the influence of the top-ranked nodes using our proposed EWNC approach and other existing weighted centrality measures. Generally, we observed that initial infected nodes are ranked top by our EWNC approach are effectively infected by other nodes in the network when compared to other centralities. In term of identification of the influential nodes in the network, our EWNC approach outperforms others centrality measures. As mentioned above, our EWNC approach is based on modification of traditional centrality measures described in Section Materials and methods, therefore, the nodes are ranked based on the interconnectivity score calculation of each pair of nodes and the number of shared neighbourhood which take into consideration the number edges (node degree) and the shortest paths between pair of nodes in a given network for calculation of weighted centrality score and the definition ϕ inherit the concept of EWNC, computing the number of shared neighborhood and the number edges associated with to a particular node to calculate the node interconnectivity difference. As shown in our formulation,

the centrality scores are based on modification of traditional centrality measures. When ranking nodes, both the degree of the node based on edges and the shortest paths between nodes are taken into account in calculation of weighted centrality score value and the definition of ϕ inherits the idea of EFCM, removing a node and the edges associated with it to calculate the difference. Based on this our EWNC approach is able to take into account the global structure of the network which make our approach more efficient compared to the classical centrality measures hence suitable for wide application of identification of influential nodes in complex networks.

Network pharmacology simulation

Recently, network science have gained wide application in medical and drug discovery research (Newaz 2022). Network pharmacology and system biology paradigm an application of network science have provided a breakthrough in drug discovery research by establishing the relationship between drug molecules and disease (Zhao et al. 2022). Discovery and development of multi-target therapeutic drug compounds with minimal or no adverse effects is exigent in treatment of complex diseases compared mono-therapeutic drug compounds (Lannes-Vieira 2022). Study has shown herbal medicine to have combinatory drug therapeutic properties hence suitable for developing multi-target therapeutics drug compounds with minimal or no adverse effects (Lannes-Vieira 2022). In this study we develop an efficient weighted network centrality approach to explore the mechanism of *Ruellia* herbal formula in the treatment of the rheumatoid arthritis. To archive this we built three distinct networks those includes (1) herb-compositive compound-putative target network; (2) herb-putative target-known RA therapeutic target network; and (3) herb-putative targets-known RA therapeutic targets-other human PPI network. All the three networks were merged to built a imbalance multi-level network in odder to identify and explore the mechanism of action of *Ruellia* herbal compounds and corresponding putative targets. We applied our new weighted centrality approach to identify influential nodes (important components) in the network to establish the mechanism of action in the treatment of the rheumatoid arthritis. According to the network analysis result we discovered a total of 57 influential nodes those includes: 8 compositive compounds, 15 putative targets, 10 RA therapeutic targets and 24 other human proteins interacting with putative targets which had high weighted centrality score values. To validated the clinical importance of the identified putative targets, an Gene Ontology and Pathway enrichment analysis were performed. From the analysis we discovered that majority of the putative targets were frequently involved in Cytokine receptor binding, Chemokine receptor binding, CXCR chemokine receptor binding,CCR2 chemokine receptor binding, CXCR chemokine receptor binding, IL-17 signaling,IL-10 signaling, TNF signaling, IL-4 and IL-13 signaling, Toll-like receptor signaling signaling pathway, NF-kappa B signaling, NOD-like receptor signaling pathway, Chemokine signaling pathway, and GPCR ligand binding which plays an important role in the progression of rheumatoid arthritis disease. Study has shown that inflammatory cytokines such as IL-6, IL-1β and TNF play a important role in triggering the catabolism and anabolism of the joints (Kato et al. 2014). IL-1β has been reported to activate the inflammatory response

by increasing the MMPs expression which play a critical role in the in the degradation of cartilage in rheumatoid arthritis (Dinarello et al. 2002). IL-6 also have been implicated with inflammatory triggered by response by producing the transcription factors such as in inflammation pathways (Kim et al. 2015). TNF is a potent anti-inflammatory cytokines that has been implicated in various autoimmune and inflammatory disease such as rheumatoid arthritis disease (Chen et al. 2022). Study has shown that two risk factors linked arthritis disease are inflammation and pain which are related to PGHS1 which is the main enzyme that regulate PGE2 synthesis that play a critical role in the inflammatory response by stimulation of the inflammatory cytokines like IL-1β and TNF-α (Glauser 1996). In addition, Nitric oxide has also been to impacted to induce mechanical stress and inflammation by modulating cytokine expression that activate MMPs, and suppress proteoglycan synthesis hence leading to pathogeneisis of rheumatoid arthritis (Guilak et al. 2004). In addition, study has also shown that systhesis of nitric oxide by inducible nitric oxide synthase plays an important role in the regulation of rheumatoid arthritis (Abramson 2008). Thus therapeutic intervention such as the use of inhibitors like N6-(1-iminoethyl)-L-lysine hydrochloride and Smethylisothiourea has been recommended in the management of rheumatoid arthritis (Balaganur et al. 2014).

To establish the suitable candidate drug compound among the 8 major compounds identified from the multi-level imbalance network, a molecular docking simulation was performed. From the docking analysis, compounds with highest binding affinity were selected (binding energy ≥ -8.0 kcal/mol and RMSD ≤ 2.5 Å). Also we selected six potential major protein targets (TNF, iNOSs, IL-1β, PTGS1, IL-6, PTGS2,DOP, CCR5 and CB2) associated with rheumatoid arthritis. Overally docking results revealed that Glyceryl diacetate-2-Oleate and Oleoyl chloride had highest binding affinity i.e. ≥ -8.0 kcal/mol to all the major protein targets. This implies the two compounds are good inhibitors of the six selected major protein targets associated with rheumatoid arthritis. In addition, Glyceryl diacetate-2-Oleate and Oleoyl chloride showed good H-bond interaction with amino residues of six selected major protein targets validating their inhibitory characteristics. We also observed that Oleoyl chloride and Glyceryl diacetate-2-Oleate were within the Lipinski limits a clear indication that their drug-likeliness properties. ADMET evaluation confirmed that both compounds may be less or not toxic to human and may not trigger DILI, H-HT or act as hERG Blockers. Study has reported drug compounds that trigger DILI and H-HT may cause adverse liver damage to patients (Andrade et al. 2019).

Conclusions

In this study we introduce an efficient weighted network centrality approach by modification of classical centrality measures using node interconnectivity. We then apply our proposed approach to explore the mechanism of action *Ruellia* herbal formula in the treatment of rheumatoid arthritis. We use the SI model was used to evaluate the node spreading process in four real networks by compared cumulative number of infected nodes using our proposed EWNC approach and other existing weighted centrality measures. The results indicated that initial infected nodes are ranked top by our EWNC approach are effectively infected by other nodes in the network when compared to other centralities. Also our EWNC approach outperforms others

centrality measures in terms of identification of the influential nodes in the network. Network pharmacology application reveled that using our approach was efficient in identification of important nodes in the network. From imbalance multi-level network analysis we discovered a total of 57 influential nodes those includes: 8 compositive compounds, 15 putative targets, 10 RA therapeutic targets and 24 other human proteins interacting with putative targets which had high weighted centrality score values. Gene Ontology and Pathway enrichment analysis confirmed that majority of the major identified putative targets were frequently in biological processed, molecular function and pathway system that plays an important role in the progression of rheumatoid arthritis disease. Molecular docking simulations indicate that four major candidate compositive compounds significant binding affinity to the selected major protein targets. Among the four compounds Glyceryl diacetate-2-Oleate and Oleoyl chloride had the highest binding energy and showed good H-bond interaction with amino residues of six selected major protein targets. The two compounds were also within the Lipinski limits a clear indication that their drug-likeliness properties. ADMET evaluation confirmed that both compounds had minimal or no toxic effect human and may not trigger DILI, H-HT or act as hERG Blockers hence indicating their potential as candidate drug compounds for treating rheumatoid arthritis. The our new weighted centrality approach provide an essential tool that may utilised to explore mechanism of action of drug compounds in the treatment of a particular disease. Our network pharmacology findings provide promising results that could lead us to design and discover of alternative drug compounds for the management and treatment of rheumatoid arthritis. Though our approach is a purely in silico method, clinical experiments are required to test and validate the hypotheses of our computational methods.

Supplementary Information

The online version contains supplementary material available at https://doi.org/10.1007/s41109-022-00527-2.

Additional file 1 This file contains *Ruellia* Contain all data used for network pharmacology studies.

Additional file 2 Contains network analysis, Gene Ontology and Pathway enrichment analysis, and molecular docking simulationsupplementary results.

Additional file 3 This file contains the all figures used in this article.

Acknowledgements
The authors acknowledge the support of National Research, Development and Innovation Office, within the framework of the Artificial Intelligence National Laboratory Programme (MILAB) RRF-2.3.1-21-2022-00004. Project No. TKP2021-NVA-09, Ministry of Innovation and Technology of Hungary, National Research, Development and Innovation Office. M. K. gratefully acknowledges the European Commission for funding the InnoRenew CoE project (Grant Agreement No. 739574) under the Horizon2020 Widespread-Teaming program and the Republic of Slovenia (Investment funding of the Republic of Slovenia and the European Union of the European Regional Development Fund). He is also grateful for the support of the Slovenian Research Agency (ARRS) through Grant N2-0171.

Author contributions
JD, PJO and MK conceived the idea and formulated the new weighted network centrality measures. AH contributed to the data collection and curation. PJO analysed the data, implemented the model, computational framework and methodology, and performed the experiments. JD and MK evaluated the experiments. All authors discussed the results and contributed to the writing of the original draft manuscript. All authors read and approved the final manuscript.

Funding
Open access funding provided by University of Szeged.

Availability of data and materials
The source code and data sets are available at https://github.com/.

Declarations

Competing interests
The authors declare that they have no competing interests.

Received: 23 October 2022 Accepted: 16 December 2022
Published online: 24 January 2023

References

Abramson SB (2008) Nitric oxide in inflammation and pain associated with osteoarthritis. Arthritis Res Ther 10(2):1–7
Agarwal S, Mehrotra R (2016) An overview of molecular docking. JSM Chem 4(2):1024–1028
Allen FH, Motherwell WS (2002) Applications of the Cambridge structural database in organic chemistry and crystal chemistry. Acta Crystallogr B 58(3):407–422
Amberger JS, Bocchini CA, Scott AF, Hamosh A (2019) Omim. org: leveraging knowledge across phenotype-gene relationships. Nucleic Acids Res 47(D1):1038–1043
Anderson J, Caplan L, Yazdany J, Robbins ML, Neogi T, Michaud K, Saag KG, O'dell JR, Kazi S (2012) Rheumatoid arthritis disease activity measures: American college of rheumatology recommendations for use in clinical practice. Arthritis Care Res 64(5):640–647
Andrade RJ, Chalasani N, Björnsson ES, Suzuki A, Kullak-Ublick GA, Watkins PB, Devarbhavi H, Merz M, Lucena MI, Kaplowitz N et al (2019) Drug-induced liver injury. Nat Rev Dis Primers 5(1):1–22
Aoki KF, Kanehisa M (2005) Using the KEGG database resource. Curr Protoc Bioinform 11(1):1–12
Arirudran B, Saraswathy A, Krishnamurthy V (2011) Antimicrobial activity of *Ruellia tuberosa* l. (whole plant). Pharmacogn J 3(23):91–95
Balaganur V, Pathak NN, Lingaraju MC, More AS, Latief N, Kumari RR, Kumar D, Tandan SK (2014) Chondroprotective and anti-inflammatory effects of s-methylisothiourea, an inducible nitric oxide synthase inhibitor in cartilage and synovial explants model of osteoarthritis. J Pharm Pharmacol 66(7):1021–1031
Beuming T, Skrabanek L, Niv MY, Mukherjee P, Weinstein H (2005) Pdzbase: a protein–protein interaction database for PDZ-domains. Bioinformatics 21(6):827–828
Brandes U (2001) A faster algorithm for betweenness centrality. J Math Sociol 25(2):163–177
Bridgewood C, Wittmann M, Macleod T, Watad A, Newton D, Bhan K, Amital H, Damiani G, Giryes S, Bragazzi NL, et al (2022) Th2 IL-4/IL-13 dual blockade with Dupilumab is linked to some emergent th17 type diseases including seronegative arthritis, enthesitis/enthesopathy, but not humoral autoimmune diseases. J Investig Dermatol
Brown KR, Jurisica I (2005) Online predicted human interaction database. Bioinformatics 21(9):2076–2082
Cao J, Ni Y, Zhang H, Ning X, Qi X (2022) Inhibition of Kruppel-like factor 7 attenuates cell proliferation and inflammation of fibroblast-like synoviocytes in rheumatoid arthritis through NF-κb and MAPK signaling pathway. Exp Anim 21–0200
Chakravarty K, McDonald H, Pullar T, Taggart A, Chalmers R, Oliver S, Mooney J, Somerville M, Bosworth A, Kennedy T (2008) BSR/BHPR guideline for disease-modifying anti-rheumatic drug (DMARD) therapy in consultation with the British Association of Dermatologists. Rheumatology 47(6):924–925
Chen D-Y, Lin C-H, Chen H-H, Tang K-T (2022) Association of tumor necrosis factor-α inhibitors and liver cirrhosis in patients with rheumatoid arthritis: a nationwide population-based nested case-control study. Int J Rheum Dis
Chen X, Li H, Tian L, Li Q, Luo J, Zhang Y (2020) Analysis of the physicochemical properties of acaricides based on Lipinski's rule of five. J Comput Biol 27(9):1397–1406
Cheng H, Guo P, Su T, Jiang C, Zhu Z, Wei W, Zhang L, Wang Q (2022) G protein-coupled receptor kinase type 2 and β-arrestin2: key players in immune cell functions and inflammation. Cell Signal 110337
Chothani DL, Patel MB, Mishra SH (2010) Review on *Ruellia tuberosa* (cracker plant). Pharmacogn J 2(12):506–512
Clark DE, Pickett SD (2000) Computational methods for the prediction of 'drug-likeness'. Drug Discov Today 5(2):49–58
Cosconati S, Forli S, Perryman AL, Harris R, Goodsell DS, Olson AJ (2010) Virtual screening with AutoDock: theory and practice. Expert Opin Drug Discov 5(6):597–607
de Freitas RA, Lima VV, Bomfim GF, Giachini FR: Interleukin-10 in the vasculature: pathophysiological implications. Curr Vasc Pharmacol (2022)
DeLano WL et al (2002) Pymol: an open-source molecular graphics tool. CCP4 Newsl Protein Crystallogr 40(1):82–92
Dennis G, Sherman BT, Hosack DA, Yang J, Gao W, Lane HC, Lempicki RA (2003) David: database for annotation, visualization, and integrated discovery. Genome Biol 4(9):1–11
Deshpande N, Addess KJ, Bluhm WF, Merino-Ott JC, Townsend-Merino W, Zhang Q, Knezevich C, Xie L, Chen L, Feng Z et al (2005) The RCSB protein data bank: a redesigned query system and relational database based on the mmCIF schema. Nucleic Acids Res 33(1):233–237
D'Eustachio, P.: Reactome knowledgebase of human biological pathways and processes. In: Bioinformatics for comparative proteomics. Springer, pp 49–61 (2011)
Dinarello CA et al (2002) The IL-1 family and inflammatory diseases. Clin Exp Rheumatol 20(5):1–13
Dogan Z, Telli G, Tel BC, Saracoglu I (2022) *Scutellaria brevibracteata* stapf and active principles with anti-inflammatory effects through regulation of NF-κB/COX-2/iNOS pathways. Fitoterapia 158:105159
Dong J, Wang N-N, Yao Z-J, Zhang L, Cheng Y, Ouyang D, Lu A-P, Cao D-S (2018) ADMETlab: a platform for systematic ADMET evaluation based on a comprehensively collected ADMET database. J Cheminform 10(1):1–11
Dörpinghaus J, Weil V, Düing C, Sommer MW (2022) Centrality measures in multi-layer knowledge graphs. arXiv:2203.09219
Ertl P, Rohde B, Selzer P (2000) Fast calculation of molecular polar surface area as a sum of fragment-based contributions and its application to the prediction of drug transport properties. J Med Chem 43(20):3714–3717

Fei L, Mo H, Deng Y (2017) A new method to identify influential nodes based on combining of existing centrality measures. Mod Phys Lett B 31(26):1750243
Feinstein WP, Brylinski M (2015) Calculating an optimal box size for ligand docking and virtual screening against experimental and predicted binding pockets. J Cheminform 7(1):1–10
Fox RI (1993) Mechanism of action of hydroxychloroquine as an antirheumatic drug. In: Seminars in arthritis and rheumatism, vol 23. Elsevier, pp 82–91
Francis P, Chakraborty K (2022) Undescribed anti-inflammatory Thalysiaketides from marine sponge *Clathria* (*thalysias*) *vulpina* (Lamarck, 1814). Chem Biodivers
Freeman LC (1978) Centrality in social networks conceptual clarification. Soc Netw 1(3):215–239
Glauser MP (1996) The inflammatory cytokines. Drugs 52(2):9–17
Grove ML, Hassell AB, Hay EM, Shadforth MF (2001) Adverse reactions to disease-modifying anti-rheumatic drugs in clinical practice. Qjm 94(6):309–319
Guilak F, Fermor B, Keefe FJ, Kraus VB, Olson SA, Pisetsky DS, Setton LA, Weinberg JB (2004) The role of biomechanics and inflammation in cartilage injury and repair. Clin Orthop Relat Res® 423:17–26
Hamri S, Bouchaour T, Lerari D, Bouberka Z, Supiot P, Maschke U (2022) Cleaning of wastewater using crosslinked poly (acrylamide-co-acrylic acid) hydrogels: analysis of rotatable bonds, binding energy and hydrogen bonding. Gels 8(3):156
Hazlewood GS, Barnabe C, Tomlinson G, Marshall D, Devoe DJ, Bombardier C (2016) Methotrexate monotherapy and methotrexate combination therapy with traditional and biologic disease modifying anti-rheumatic drugs for rheumatoid arthritis: a network meta?analysis. Cochrane Database Syst Rev 8
Hodgens A, Sharman T (2021) Corticosteroids. In: StatPearls [Internet]. StatPearls Publishing
Huey R, Morris GM, Olson AJ, Goodsell DS (2007) A semiempirical free energy force field with charge-based desolvation. J Comput Chem 28(6):1145–1152
Iacobucci D, McBride R, Popovich D (2017) Eigenvector centrality: illustrations supporting the utility of extracting more than one eigenvector to obtain additional insights into networks and interdependent structures. J Soc Struct 18(2):1–22
Kapugi M, Cunningham K (2019) Corticosteroids. Orthop Nurs 38(5):336–339
Kato T, Miyaki S, Ishitobi H, Nakamura Y, Nakasa T, Lotz MK, Ochi M (2014) Exosomes from IL-1β stimulated synovial fibroblasts induce osteoarthritic changes in articular chondrocytes. Arthritis Res Ther 16(4):1–11
Kelleni M (2021) Potential crucial role of COX-1 and/or COX-2 inhibition, NSAIDs or aspirin triggered lipoxins and resolvins in amelioration of COVID-19 mortality
Kerrien S, Aranda B, Breuza L, Bridge A, Broackes-Carter F, Chen C, Duesbury M, Dumousseau M, Feuermann M, Hinz U et al (2012) The intact molecular interaction database in 2012. Nucleic Acids Res 40(D1):841–846
Kim GW, Lee NR, Pi RH, Lim YS, Lee YM, Lee JM, Jeong HS, Chung SH (2015) IL-6 inhibitors for treatment of rheumatoid arthritis: past, present, and future. Arch Pharmacal Res 38(5):575–584
Kim S, Thiessen PA, Bolton EE, Chen J, Fu G, Gindulyte A, Han L, He J, He S, Shoemaker BA et al (2016) Pubchem substance and compound databases. Nucleic Acids Res 44(D1):1202–1213
Koller G, Cusnir I, Hall J, Ye C (2019) Reversible alopecia areata: a little known side effect of leflunomide. Clin Rheumatol 38(7):2015–2016
Koper-Lenkiewicz OM, Sutkowska K, Wawrusiewicz-Kurylonek N, Kowalewska E, Matowicka-Karna J (2022) Proinflammatory cytokines (IL-1,-6,-8,-15,-17,-18,-23, TNF-α) single nucleotide polymorphisms in rheumatoid arthritis—a literature review. Int J Mol Sci 23(4):2106
Kour G, Choudhary R, Anjum S, Bhagat A, Bajaj BK, Ahmed Z (2022) Phytochemicals targeting JAK/STAT pathway in the treatment of rheumatoid arthritis: Is there a future? Biochem Pharmacol 197:114929
Kremer JM, Alarcón GS, Lightfoot RW Jr, Willkens RF, Furst DE, Williams HJ, Dent PB, Weinblatt ME (1994) Methotrexate for rheumatoid arthritis. Arthritis Rheum 37(3):316–328
Kuhn M, von Mering C, Campillos M, Jensen LJ, Bork P (2007) Stitch: interaction networks of chemicals and proteins. Nucleic Acids Res 36(1):684–688
Lannes-Vieira J (2022) Multi-therapeutic strategy targeting parasite and inflammation-related alterations to improve prognosis of chronic Chagas cardiomyopathy: a hypothesis-based approach. Memórias do Instituto Oswaldo Cruz 117
Laskowski RA, Swindells MB (2011) LigPlot+: multiple ligand–protein interaction diagrams for drug discovery. ACS Publications
Lehne B, Schlitt T (2009) Protein–protein interaction databases: keeping up with growing interactomes. Hum Genomics 3(3):1–7
Li R, Ma Y, Hong J, Ding Y (2022) Nanoengineered therapy aiming at the etiology of rheumatoid arthritis. Nano Today 42:101367
Licata L, Briganti L, Peluso D, Perfetto L, Iannuccelli M, Galeota E, Sacco F, Palma A, Nardozza AP, Santonico E et al (2012) Mint, the molecular interaction database: 2012 update. Nucleic Acids Res 40(D1):857–861
Martin RW, McCallops K, Head AJ, Eggebeen AT, Birmingham JD, Tellinghuisen DJ (2013) Influence of patient characteristics on perceived risks and willingness to take a proposed anti-rheumatic drug. BMC Med Inform Decis Mak 13(1):1–9
Mogul A, Corsi K, McAuliffe L (2019) Baricitinib: the second FDA-approved JAK inhibitor for the treatment of rheumatoid arthritis. Ann Pharmacother 53(9):947–953
Molinspiration C (2011) Calculation of molecular properties and bioactivity score. http://www.molinspiration.com/cgi-bin/properties
Morris GM, Huey R, Olson AJ (2008) Using AutoDock for ligand-receptor docking. Curr Protoc Bioinform 24(1):8–14
Newaz K (2022) Novel network science approaches for a better understanding of protein folding and human aging. University of Notre Dame
Newman ME (2001) Scientific collaboration networks. II. Shortest paths, weighted networks, and centrality. Phys Rev E 64(1):016132

Newman ME (2001) Clustering and preferential attachment in growing networks. Phys Rev E 64(2):025102
Nickel J, Gohlke B-O, Erehman J, Banerjee P, Rong WW, Goede A, Dunkel M, Preissner R (2014) SuperPred: update on drug classification and target prediction. Nucleic Acids Res 42(W1):26–31
Niu W-H, Wu F, Cao W-Y, Wu Z-G, Chao Y-C, Peng F, Liang C (2021) Network pharmacology for the identification of phytochemicals in traditional Chinese medicine for COVID-19 that may regulate interleukin-6. Biosci Rep 41(1)
Nogales C, Mamdouh ZM, List M, Kiel C, Casas AI, Schmidt HH (2021) Network pharmacology: curing causal mechanisms instead of treating symptoms. Trends Pharmacolog Sci
O'Boyle NM, Banck M, James CA, Morley C, Vandermeersch T, Hutchison GR (2011) Open babel: an open chemical toolbox. J Cheminform 3(1):1–14
Özgür A, Vu T, Erkan G, Radev DR (2008) Identifying gene-disease associations using centrality on a literature mined gene-interaction network. Bioinformatics 24(13):277–285
Prasad T, Kandasamy K, Pandey A (2009) Human protein reference database and human proteinpedia as discovery tools for systems biology. In: Reverse chemical genetics. Springer, pp 67–79
Raucci F, Saviano A, Casillo GM, Guerra-Rodriguez M, Mansour AA, Piccolo M, Ferraro MG, Panza E, Vellecco V, Irace C et al (2022) IL-17-induced inflammation modulates the mPGES-1/PPAR-γ pathway in monocytes/macrophages. Br J Pharmacol 179(9):1857–1873
Reia SM, Herrmann S, Fontanari JF (2017) Impact of centrality on cooperative processes. Phys Rev E 95(2):022305
Rodrigues FA, Peron TKD, Ji P, Kurths J (2016) The Kuramoto model in complex networks. Phys Rep 610:1–98
Scherer HU, Häupl T, Burmester GR (2020) The etiology of rheumatoid arthritis. J Autoimmun 110:102400
Skrzypkowska M, Stasiak M, Sakowska J, Chmiel J, Maciejewska A, Buciński A, Słomiński B, Trzonkowski P, Łuczkiewicz P (2022) Cytokines and chemokines multiplex analysis in patients with low disease activity rheumatoid arthritis. Rheumatol Int 42(4):609–619
Smolen J, Breedveld F, Schiff M, Kalden J, Emery P, Eberl G, Van Riel P, Tugwell P (2003) A simplified disease activity index for rheumatoid arthritis for use in clinical practice. Rheumatology 42(2):244–257
Swain N, Tripathy A, Padhan P, Raghav SK, Gupta B (2022) Toll-like receptor-7 activation in CD8+ T cells modulates inflammatory mediators in patients with rheumatoid arthritis. Rheumatol Int 1–11
Szklarczyk D, Gable AL, Nastou KC, Lyon D, Kirsch R, Pyysalo S, Doncheva NT, Legeay M, Fang T, Bork P et al (2021) The string database in 2021: customizable protein-protein networks, and functional characterization of user-uploaded gene/measurement sets. Nucleic Acids Res 49(D1):605–612
Tóth L, Juhász MF, Szabó L, Abada A, Kiss F, Hegyi P, Farkas N, Nagy G, Helyes Z (2022) Janus kinase inhibitors improve disease activity and patient reported outcomes in rheumatoid arthritis: a systematic review and meta-analysis of 24,135 patients. Int J Mol Sci 23(3):1246
Veber DF, Johnson SR, Cheng H-Y, Smith BR, Ward KW, Kopple KD (2002) Molecular properties that influence the oral bioavailability of drug candidates. J Med Chem 45(12):2615–2623
Wachi S, Yoneda K, Wu R (2005) Interactome-transcriptome analysis reveals the high centrality of genes differentially expressed in lung cancer tissues. Bioinformatics 21(23):4205–4208
Wan Y, Xu L, Liu Z, Yang M, Jiang X, Zhang Q, Huang J (2019) Utilising network pharmacology to explore the underlying mechanism of Wumei pill in treating pancreatic neoplasms. BMC Complement Altern Med 19(1):1–12
Wang S, Du Y, Deng Y (2017) A new measure of identifying influential nodes: efficiency centrality. Commun Nonlinear Sci Numer Simul 47:151–163
Wang Y, Zhang S, Li F, Zhou Y, Zhang Y, Wang Z, Zhang R, Zhu J, Ren Y, Tan Y et al (2020) Therapeutic target database 2020: enriched resource for facilitating research and early development of targeted therapeutics. Nucleic Acids Res 48(D1):1031–1041
Weyand CM, Goronzy JJ (2021) The immunology of rheumatoid arthritis. Nat Immunol 22(1):10–18
Wishart DS, Feunang YD, Guo AC, Lo EJ, Marcu A, Grant JR, Sajed T, Johnson D, Li C, Sayeeda Z, Assempour N (2018) DrugBank 5.0: a major update to the DrugBank database for 2018. Nucleic Acids Res 46(D1):1074–1082
Xin W, Zi-Yi W, Zheng J-H, Shao L (2021) TCM network pharmacology: a new trend towards combining computational, experimental and clinical approaches. Chin J Nat Med 19(1):1–11
Xiong G, Wu Z, Yi J, Fu L, Yang Z, Hsieh C, Yin M, Zeng X, Wu C, Lu A et al (2021) ADMETlab 2.0: an integrated online platform for accurate and comprehensive predictions of ADMET properties. Nucleic Acids Res 49(1):5–14
Xu X, Zhang W, Huang C, Li Y, Yu H, Wang Y, Duan J, Ling Y (2012) A novel chemometric method for the prediction of human oral bioavailability. Int J Mol Sci 13(6):6964–6982
Yu G, Wang W, Wang X, Xu M, Zhang L, Ding L, Guo R, Shi Y (2018) Network pharmacology-based strategy to investigate pharmacological mechanisms of Zuojinwan for treatment of gastritis. BMC Complement Altern Med 18(1):1–12
Yuan C, Wang M-H, Wang F, Chen P-Y, Ke X-G, Yu B, Yang Y-F, You P-T, Wu H-Z (2021) Network pharmacology and molecular docking reveal the mechanism of scopoletin against non-small cell lung cancer. Life Sci 270:119105
Zhang M-Q, Wilkinson B (2007) Drug discovery beyond the rule-of-five. Curr Opin Biotechnol 18(6):478–488
Zhao J, Song Y, Deng Y (2020) A novel model to identify the influential nodes: evidence theory centrality. IEEE Access 8:46773–46780
Zhao Z, Wang L, Zhang M, Zhou C, Wang Y, Ma J, Fan Y (2022) Reveals of quercetins therapeutic effects on oral lichen planus based on network pharmacology approach and experimental validation. Sci Rep 12(1):1–13
Zhou T, Liu J-G, Bai W-J, Chen G, Wang B-H (2006) Behaviors of susceptible-infected epidemics on scale-free networks with identical infectivity. Phys Rev E 74(5):056109
Zhou Z, Chen B, Chen S, Lin M, Chen Y, Jin S, Chen W, Zhang Y (2020) Applications of network pharmacology in traditional Chinese medicine research. Evid Based Complement Altern Med 2020

Publisher's Note